IDŐJÁRÁS

QUARTERLY JOURNAL
OF THE HUNGARIAN METEOROLOGICAL SERVICE

CONTENTS

****

http://www.met.hu/firat/ido-e.html

VOL. 102 * NO. 2 * APRIL–JUNE 1998

IDŐJÁRÁS

Quarterly Journal of the Hungarian Meteorological Service

Editorial Office: P.O. Box 39, H-1675 Budapest, Hungary or
Gilice tér 39, H-1181 Budapest, Hungary
E-mail: gmajor@met.hu or *antal@met.hu*
Fax: (36-1) 290-7387

Subscription by

mail: IDŐJÁRÁS, P.O. Box 39, H-1675 Budapest, Hungary;
E-mail: gmajor@met.hu or *antal@met.hu*; *Fax: (36-1) 290-7387*

IDŐJÁRÁS

Quarterly Journal of the Hungarian Meteorological Service
Vol. 102, No. 2, April–June 1998, pp. 71–107

On the origin of model errors. Part II. Effects of the spatial discretization for Hamiltonian systems

Barbara Kádár, István Szunyogh[1]

Department of Meteorology, Eötvös Loránd University,
H-1083 Budapest, Ludovika tér 2, Hungary
E-mail: kadar@nimbus.elte.hu

and **Dezső Dévényi**

NOAA/ERL/Forecast Systems Laboratory,
325 Broadway, Boulder CO, USA; E-mail: devenyi@fsl.noaa.gov
also affiliated with
Cooperative Institute for Research in Environmental Sciences,
University of Colorado at Boulder, Boulder, CO, USA

(Manuscript received 2 December 1997; in final form 12 March 1998)

Abstract—The effects of model errors stemming from the temporal and spatial discretizations of the continuous model equations are investigated (in two parts) for Hamiltonian systems. In this second part of the paper the effects of spatial truncation are discussed. Since the "article relabelling" symmetry is only implicit in the Eulerian description, the spatial truncation of the Eulerian equations inevitably distorts the individual conservation properties of the flow. Theoretical considerations and numerical experiments confirm that the wave mode interactions misrepresented in the finite dimensional truncation are responsible for the destruction of structure and the breaking of conservation laws. Although there is no way to circumvent this problem, there are two approaches to reduce the effects of the falsely represented interactions: (1) Increasing the resolution and initializing the fields so that the energy of high wavenumber modes is small; (2) Use of structure preserving schemes that can conserve the algebraic structure and a finite number of invariants. To illustrate these methods the results of numerical experiments carried out with a traditional (aliased) and a structure preserving truncation of the two-dimensional vorticity equation and of the 2-layer quasi-geostrophic model are presented.

Key-words: Hamiltonian formalism, invariants of motion, structure preserving spatial truncation.

---

[1] Present affiliation: UCAR scientific visitor at the National Centers for Environmental Prediction, USA; E-mail: Istvan.Szunyogh@noaa.gov

1. Introduction

In the first part of this paper (*Kádár et al.*, 1998, hereafter Part I) we discussed the effects of temporal discretizations. We pointed out, that even if the spatially discretized equations were perfect, the time integration inevitably introduces model errors whose effects in a chaotic system lead to the complete loss of the forecast skill within a finite time interval. This part concentrates on the effect of spatial discretizations and as in Part I we start considering conservative fluid dynamical processes.

Atmospheric (fluid) dynamics is based on the classical mechanical model of interacting atmospheric (fluid) particles. The number of these particles is infinite and their volume goes to zero in a mathematical analytical sense. The infinite dimensional system of equations describing the motion of the particles is called the Lagrangian form of the atmospheric (fluid) dynamical equations. These equations, however, are very rarely used for either the solution of theoretical problems or for more practice oriented forecasting purposes.

Our main interest is usually in predicting the state of the atmosphere at given geographical locations. This goal can be achieved by solving the Eulerian form of the dynamical equations, where we do not distinguish between the individual fluid particles any more. One should always keep in mind, however, that the fundamental physical model even in the case of the Eulerian equations is the one utilizing infinitesimal fluid particles. The ultimate test of any numerical solution strategy is to examine to what extent it can preserve the fundamental properties associated with the system of particles. The main difficulty with investigating the effects of spatial discretization of the Eulerian equations stems from the fact that it discretizes the space instead of the fluid and we cannot speak about fluid particles any more. This problem is more than a simple technical difficulty. Examination of the rigid body equations provided guidance for exploring the relations between the Eulerian and the Lagrangian characteristics of fluid motions (see *Arnold*, 1989, App. 2). The key step in this procedure is the identification of a metric naturally arising from the equations themselves. Once the equations are discretized in space the choice of this metric is not apparent any more (*Zeitlin* and *Pasmanter*, 1994). The discussion of this important theoretical problem is out of the scope of the present paper, but the paper by *Dowker* and *Wolski* (1992), though fails to give definite answer, gives an insight into the technical and theoretical difficulties associated with this problem. Here we follow the traditional, technically less demanding approach, i.e. we will investigate quantitative properties directly related to the original physical model which are still calculable in the discretized Eulerian systems. Conservation laws offer a unique opportunity to realize this program.

Lagrangian forms of the adiabatic primitive equations ensure the individual (particle) conservation of (potential-)vorticity-type quantities in addition to the usual mechanical invariants, such as total energy and momenta of the system.

Noether's theorem (*Olver*, 1989; *Shepherd*, 1990) connects the individual conservations to the "relabelling" symmetry: interchanging particles of the same (potential-)vorticity does not alter the motion of the system. Derivation of Eulerian equations is a reduction via these symmetries. Neither the replacement of particles along the isolines of individual invariants nor the symmetries themselves can be detected in the Eulerian description. Remarkably however, Hamiltonian mechanics provides a systematic way to find the so-called Casimir invariants associated with hidden symmetries.

Dealing with the conservative part of the equations governing fluid motions, we make use of this advantage of Hamiltonian formalism. In Section 2 we briefly summarize the invariants of motions of Hamiltonian systems. Since the effects of the different truncation methods on these conservation laws are in the forefront of our interest, in Section 3 we describe the criteria for maintaining the conservation laws in the spatial discretization of the continuous equations.

Section 4 contains the description of a traditional and a structure conserving spectral truncation of the two-dimensional vorticity equation on a double periodic plane. The continuous equation has infinite invariants of motion — reflecting the individual conservation of vorticity. We examine how the traditional discretization methods distort the algebraic structure of the original continuous equation and break most conservation laws. The structure preserving truncation does retain the Hamiltonian structure and preserve a finite number of invariants, but these are not identical with the discrete analogues of the original integrals of motion.

The quasi-geostrophic layer models, which are important tools for investigating baroclinic instability in geophysical fluids since they are capable to simulate baroclinic phenomena even at very low resolution, also possess Hamiltonian structure (*McLachlan et al.*, 1997). Since the truncation methods used for the two-dimensional vorticity equation are applicable to these models as well, the comparative study was extended to these more realistic models. Section 5 describes the basic equations and the applied truncation strategies to these models.

Fortunately, there is a remarkably efficient integration algorithm that can be used for the integration of both truncations of the vorticity equation and the quasi-geostrophic layer models (*McLachlan*, 1993). It makes feasible to carry out even extremely long numerical integrations. The role of the constraints exerted by the additional invariants conserved in the structure preserving truncation were investigated through numerical experiments. The results are presented in Section 6. Summary and conclusions are given in Section 7.

There are several statements in the main body of the paper about the structure and the conservation laws of the schemes. Since the authors tried to use the standard mathematical tools and methods of the meteorological literature in the verification of these statements, the proofs are sometimes a bit cumbersome. Since the technical details of these considerations are not necessary for understanding the main points of the paper, we placed the rigorous proofs in the Appendices.

2. *Conservation laws in Hamiltonian systems*

In Part I the basis of Hamiltonian formalism was introduced. In this section the conservation laws associated with Hamiltonian systems are summarized.

2.1 Finite dimensional systems

Once a system of ordinary differential equations is cast in Hamiltonian form, i.e. the skew-symmetric structure matrix **D** and the Hamiltonian H is determined in a way that the Jacobi identity holds for the structure functions (see Section 3.1 in Part I), the invariants of motions can be systematically identified.

The invariance of H is ensured by the skew-symmetry of **D** since

$$\frac{dH}{dt} = (\nabla H)^T \frac{d\mathbf{x}}{dt} = (\nabla H)^T \mathbf{D} \nabla H = -(\nabla H)^T \mathbf{D} \nabla H = 0. \tag{1}$$

In other words, the Hamiltonian H is invariant with respect to translation in time. Further symmetries of H lead to other invariant quantities.

There is, however, another class of invariants, the so called *Casimirs* or *distinguished functions*, which are independent of the Hamiltonian function H (*Shepherd*, 1990). These are the solutions of the homogeneous system of equations

$$\mathbf{D} \nabla C = 0. \tag{2}$$

Their invariance follows from

$$\frac{dC}{dt} = (\nabla C)^T \mathbf{D} \nabla H = -(\nabla H)^T \mathbf{D} \nabla C = 0, \tag{3}$$

where again the skew-symmetry of **D** was taken into account. The number of independent Casimirs is equal to the dimension of the kernel of **D**.

2.2 Continuous Hamiltonian systems

In continuous Hamiltonian systems there are also two classes of invariants: those that are connected to the continuous symmetries of the Hamiltonian (e.g. the Hamiltonian itself) and the *Casimirs* that are the solutions of

$$\mathcal{D} \delta \mathcal{C} = 0. \tag{4}$$

For the two-dimensional vorticity equation (see Part I, Eq. (8)), for example, the Casimirs can be written

$$\mathcal{C} = \int_{\Omega} \mathcal{J}(\zeta) d\mathbf{x}, \tag{5}$$

where $\mathcal{J}$ is an arbitrary smooth function of the vorticity ζ (*Olver*, 1989). For the system of primitive equations and its consistent simplifications (e.g. for the quasi-geostrophic layer models) the potential vorticity is an individually conserved quantity the integrals of whose functions serve as Casimir invariants. More about the conservation laws in Hamiltonian fluid dynamical systems can be found e.g. in *Shepherd* (1990).

3. Spatial discretizations of continuous Hamiltonian systems

The solution of Eulerian atmospheric governing equations requires the application of approximating numerical methods that solve a finite dimensional algebraic analogue of the original system of partial differential equations after the spatial and temporal discretization of the meteorological fields. Schemes used in the numerical simulation of atmospheric motions, however, preserve the Hamiltonian structure only in part (*Szunyogh*, 1993). Since the conservation properties of Hamiltonian systems are closely related to their algebraic structure, this fact substantially restricts the number of retained invariants of motions.

3.1 Formal conservation of the total energy

Since the conservation of total energy is solely related to the skew-symmetry of the structure matrix, the problem of constructing a total energy conserving scheme is equivalent to deriving a skew-symmetric finite dimensional analogue of the continuous differential operator $\mathcal{D}(\mathbf{u})$. The first explorers of formally energy conserving schemes (*Lorenz*, 1960; *Arakawa*, 1966) proceeded along this line, although they did not realize the underlying Hamiltonian structure.

3.2 Formal conservation of the Casimir invariants

If the numerical structure matrix **D** is skew-symmetric, the Casimir invariants of the model are determined by the kernel of **D** (Eq. (2)). Therefore, if one attempts to construct a numerical scheme preserving the finite dimensional analogue $C(\mathbf{x})$ of a Casimir invariant $\mathcal{C}(\mathbf{u})$ of the original continuous system the entries of **D** have to be set according to Eq. (2). The existence of energy and

(potential)-enstrophy preserving schemes (e.g. *Arakawa*, 1966; *Arakawa* and *Lamb*, 1980; *Salmon* and *Talley*, 1989) demonstrates that the preservation of energy and one of the Casimirs at the same time is a realizable goal. The theoretical upper limit for the number of retained Casimir invariants, however, is equal to the corank of **D**. This suggests that an optimal scheme can preserve further Casimirs.

On the other hand, *Szunyogh* (1993) observed that the conservation of the energy (skew-symmetry of **D**) is not a necessary condition for the preservation of a prechosen Casimir. Let

$$(\nabla C)^T \mathbf{D} = 0, \tag{6}$$

then

$$\frac{dC}{dt} = (\nabla C)^T \mathbf{D} \nabla H = 0. \tag{7}$$

The quantity C is a Casimir invariant in the sense that it is independent of the energy function, but it is not a Casimir in the sense of Eq. (2) if **D** is not skew-symmetric (when **D** is skew-symmetric then Eq. (7) is equivalent to Eq. (2)). The best known examples of this type of schemes are Arakawa's enstrophy conserving schemes for the two-dimensional vorticity equation (*Arakawa*, 1966) and Sadourny's potential-enstrophy conserving scheme for the shallow-water equations (*Sadourny*, 1975).

4. Truncation strategies to the two-dimensional vorticity equation

Although the two-dimensional vorticity equation is of interest in atmospheric dynamics only when the beta-effect is negligible, i.e. when the significant scales of motions are short compared to a stationary Rossby wavelength, its capability to describe the nonlinear interactions of different scale motions makes it an extremely useful environment for testing different truncation methods. The Jacobian governs the advection of the individual invariant in the flow and the errors in the approximation of this term are related to the breaking of individual conservation laws.

In this section we describe the Hamiltonian structure of the two-dimensional vorticity equation in its spectral form and its Casimir invariants. In Subsection 2 we examine how the structure (the Jacobi identity) is destroyed by traditional truncation methods. In Subsection 3 a structure preserving truncation (the so called *sine-bracket* truncation) and its conservation properties are described.

4.1 The Hamiltonian structure of the two-dimensional vorticity equation

The two-dimensional vorticity equation on a double-periodic plane transformed with the two-dimensional Fourier transformation takes the form of an infinite system of ordinary differential equations

$$\frac{d\zeta_{\mathbf{m}}}{dt} = \sum_{\substack{n_1, n_2 = -\infty \\ \mathbf{n} \neq \mathbf{0}}}^{\infty} \frac{\mathbf{m} \times \mathbf{n}}{|\mathbf{n}|^2} \zeta_{\mathbf{m}+\mathbf{n}} \zeta_{-\mathbf{n}}. \tag{8}$$

In Eq. (8) $\zeta_{\mathbf{m}}$ denotes the spectral coefficient associated with the two-dimensional integral wave vector $\mathbf{m}$, and the skew-symmetric scalar product is $\mathbf{m} \times \mathbf{n} = m_1 n_2 - m_2 n_1$. The spectral variables satisfy the reality condition $\zeta_{\mathbf{m}} = \zeta^*_{-\mathbf{m}}$, where star denotes complex conjugate. The condition $\mathbf{n} \neq \mathbf{0}$ does not restrict generality since the circulation $\zeta_{\mathbf{0}}$ is a Casimir invariant of Eq. (8), and does not contribute to the time change of any other variable because $\mathbf{m} \times \mathbf{0} = 0$. The Hamiltonian takes the form

$$H = \frac{1}{2} \sum_{\substack{n_1, n_2 = -\infty \\ \mathbf{n} \neq \mathbf{0}}}^{\infty} \frac{\zeta_{\mathbf{n}} \zeta_{-\mathbf{n}}}{|\mathbf{n}|^2}, \tag{9}$$

while the entries of the structure matrix are

$$\mathbf{D}_{\mathbf{mn}} = \mathbf{m} \times \mathbf{n} \zeta_{\mathbf{m}+\mathbf{n}}. \tag{10}$$

The skew-symmetry of the structure matrix follows from $\mathbf{m} \times \mathbf{n} = -\mathbf{n} \times \mathbf{m}$. The Jacobi identity (see Eq. (5) in Part I) can also be shown to hold.

When periodic boundary conditions are applied, the Casimir invariants, $\mathcal{C}^N = \frac{1}{\Omega} \int_\Omega \zeta^N d\mathbf{x}$ can be expressed with the spectral coefficients as follows

$$\mathcal{C}^N = \frac{1}{\Omega} \int_\Omega \zeta^N d\mathbf{x} = \sum_{\sum_{i=1}^{N} \mathbf{n}_i = \mathbf{0}}^{N} \zeta_{\mathbf{n}_1} \cdots \zeta_{\mathbf{n}_N}. \tag{11}$$

In order to point out later the deficiencies of the truncated systems in conserving the Casimir invariants, it is worth verifying directly that Eq. (2) is valid, that is

$$\left[\mathbf{D}\frac{\partial \mathcal{C}^N}{\partial \zeta}\right]_{\mathbf{k}} = 0 \tag{12}$$

for each $\mathbf{k} \in I$. Using Eq. (10) and Eq. (11) the left-hand side of Eq. (12) reads

$$\sum_{\mathbf{i}\in I} \mathbf{D}_{\mathbf{k}\mathbf{i}} \frac{\partial \mathcal{C}^N}{\partial \zeta_{\mathbf{i}}} = N \sum_{\mathbf{i}\in I} \sum_{\substack{N-1 \\ \sum_{j=1} \mathbf{m}_j = -\mathbf{i}}} (\mathbf{k} \times (\mathbf{k}+\mathbf{i}))\, \zeta_{\mathbf{k}+\mathbf{i}}\, \zeta_{\mathbf{m}_1} \cdots \zeta_{\mathbf{m}_{N-1}} . \tag{13}$$

Note that this double sum contains every N-fold product of $\zeta_{\mathbf{n}_i}$-s in which the sum of the indices equals $\mathbf{k}$. Let us examine one particular product in this summation containing the variables $\zeta_{\mathbf{e}_1} \cdots \zeta_{\mathbf{e}_N}$, where $\sum_{i=1}^{N} \mathbf{e}_i = \mathbf{k}$. These $\zeta_{\mathbf{e}_i}$-s can be put in $N!$ different orders, and in $(N-1)!$ different orders with a particular $\zeta_{\mathbf{e}_i}$ in the first position defining the coefficient of this particular product: $\mathbf{k} \times \mathbf{e}_i$. Thus the summation above can be written

$$\sum_{\{\mathbf{e}_i\} \in P_N^{\mathbf{k}}} \zeta_{\mathbf{e}_1} \cdots \zeta_{\mathbf{e}_N} \left[(N-1)! \sum_{i=1}^{N} \mathbf{k} \times \mathbf{e}_i \right], \tag{14}$$

where $P_N^{\mathbf{k}}$ contains all subsets $\{\mathbf{m}_1, \ldots, \mathbf{m}_N\}$ of indices that obey $\sum_{i=1}^{N} \mathbf{m}_i = \mathbf{k}$ (different permutations do not add new terms to the above sum). Since

$$\sum_{i=1}^{N} \mathbf{k} \times \mathbf{e}_i = \mathbf{k} \times \left[\sum_{i=1}^{N} \mathbf{e}_i \right] = \mathbf{k} \times \mathbf{k} = 0, \tag{15}$$

Eq. (13) indeed equals 0 for all $\mathbf{k} \in I$. Note that each spectral coefficient appears in an infinite number of conservation laws, which provide infinite constraints for the individual spectral coefficients over the time evolution of the flow generated by Eq. (8).

In order to be able to integrate spectral equations the wave modes taken into account should form a finite set, that is, a finite number of equations and spectral coefficients should be considered. The components of the vector of dynamical variables are the spectral coefficients $\zeta_{\mathbf{m}}$ with $\mathbf{m}$ taking its value from the lattice $-T \le m_1, m_2 \le T$. The main difficulty is the suitable modifi-

cation of the structure functions. This modification is unavoidable because there are always index pairs **m** and **n** in the truncated system for which **m** + **n** is out of the lattice. To our knowledge there is no superior truncation strategy, the different schemes correspond to different "best fit" criteria (*Machenhauer*, 1991). The general form of the modified structure functions is

$$\mathbf{D}_{\mathbf{mn}} = C_{\mathbf{mn}}^{F(\mathbf{m},\mathbf{n})}(\mathbf{m},\mathbf{n})\,\zeta_{F(\mathbf{m},\mathbf{n})}, \tag{16}$$

where the function $F(\mathbf{m},\mathbf{n})$ takes its value from the set of the retained indices in the truncated system.

4.2 Traditional truncation strategies

Traditional truncation strategies use $F(\mathbf{m},\mathbf{n}) = \mathbf{m} + \mathbf{n}$ and $C_{\mathbf{mn}}^{F(\mathbf{m},\mathbf{n})} = \mathbf{m} \times \mathbf{n}$ if $|m_1 + n_1| \le T$, $|m_2 + n_2| \le T$ and attempt to find optimal definitions for the functions $F(\mathbf{m},\mathbf{n})$ and $C_{\mathbf{mn}}^{F(\mathbf{m},\mathbf{n})}$ if $|m_1 + n_1| > T$ or $|m_2 + n_2| > T$.

There are two basic approaches to truncate the system of equations at a wavenumber T.

4.2.1 Aliasing-free truncation

The strategy which minimizes the mean square residue, the difference between the two sides of the truncated equation, is the aliasing-free truncation (*Machenhauer*, 1991). The structure function $\mathbf{D}_{\mathbf{mn}}$ is set to zero if $|m_1 + n_1| > T$ or $|m_2 + n_2| > T$, otherwise it is defined by Eq. (10). The fact that the residue can only be minimal, but not zero, reflects the inevitable approximating character of the scheme.

4.2.2 Aliased truncation

The aliased truncation is a "best fit" strategy in the sense that all interactions between the retained wave modes are taken into consideration and the conservation of quadratic invariants is ensured. In this case $F(\mathbf{m},\mathbf{n}) = (\mathbf{m} + \mathbf{n})\, mod M$, where $M = 2T + 1$, and $\mathbf{a}\, mod M = \mathbf{b} = (b_1, b_2)$ with b_i being the least in absolute value integer congruent with a_i modulo M (i = 1,2). There are different possible choices for $C_{\mathbf{mn}}^{F(\mathbf{m},\mathbf{n})}$, a straightforward one would be $C_{\mathbf{mn}}^{F(\mathbf{m},\mathbf{n})} = [(\mathbf{m} + \mathbf{n}) mod M] \times \mathbf{n}$. A scheme with this choice, however, does not conserve the energy, because the corresponding structure matrix is not

skew-symmetric. This problem can be solved by setting $C_{\mathbf{mn}}^{F(\mathbf{m},\mathbf{n})} = (\mathbf{m} \times \mathbf{n}) mod M$. This approach also preserves the enstrophy and hereafter the notion aliased truncation corresponds to this scheme. Note that $\mathbf{D}_{\mathbf{mn}}$ is different from its original untruncated form, only if $|m_1 + n_1| > T$ or $|m_2 + n_2| > T$.

4.2.3 Structure of the traditional schemes

Both techniques have the limitation misinterpreting interactions between modes $\zeta_{\mathbf{m}}$ and $\zeta_{\mathbf{n}}$ if $|m_1 + n_1| > T$ or $|m_2 + n_2| > T$. In the aliasing-free case these interactions are neglected, while in the second case the aliased interactions affect different modes than in the untruncated equations. In the numerical practice the first approach dominates, thanks to the unambiguous results of the numerical experiments of *Orszag* (1971) and to the fact that it is a least square approximation. *Lorenz* (1960) pointed out that the aliasing-free scheme ensures the conservation of quadratic invariants, provided that all possible interactions between a triad of retained wavenumbers are taken into account, even if additional interactions are disregarded. The aliasing free truncated system in general, however, is not Hamiltonian. (For proof see Appendix A.)

Roughly speaking, the aliasing-free truncation violates the algebraic structure because it neglects numerous interactions between the components of the state vector. It suggests that the aliased truncation, which is free of the above error, may preserve the structure. Unfortunately, it is not the case. Although it also preserves the quadratic invariants, the aliased truncation for $T \geq 2$ does not satisfy the Jacobi identity, i.e. it is not Hamiltonian[2]. The maximal truncation $T = 1$ seems to be an exceptional case in the sense that it does satisfy the Jacobi identity.

A finite-difference scheme is an aliased truncated spectral scheme, though the function $C_{\mathbf{mn}}^{F(\mathbf{m},\mathbf{n})}(\mathbf{m},\mathbf{n})$ for it may have a substantially different form from what was used in this section and the structure function $\mathbf{D}_{\mathbf{mn}}$ for $|m_1 + n_1| \leq T$ and $|m_2 + n_2| \leq T$ may also be modified. Spectral transforms of energy and enstrophy conserving finite difference schemes have the property that the function $C_{\mathbf{mn}}^{F(\mathbf{m},\mathbf{n})}(\mathbf{m},\mathbf{n})$ satisfies the conditions for the preservation of quadratic invariants (for an example see the spectral form of the nine-point Arakawa Jacobian in *Bennett* and *Middleton* (1983).

---

[2] To our knowledge the fact that spectral truncation destroys the Jacobi identity was first reported by *Morrison* (1981) in a paper that seems to be forgotten. He also proposed a structure preserving truncation strategy based on the use of Clebsch potentials, but this method doubles the dimension of the space and the practical applicability of this approach has never been tested.

4.2.4 Conservation laws of traditional schemes

Since the traditional schemes conserve the quadratic invariants, the main problem is whether they can preserve the truncated analogues of the Casimir invariants $\mathcal{C}^N$ (Eq. 11) for $N > 2$. The following statement can be made about the conservation laws of traditional truncation methods: *The aliasing-free traditional truncation does not preserve the finite analogues of the Casimirs* $\mathcal{C}^N$ *for* $N > 2$ *at any resolution. (For proof see Appendix B.)* It is also true for the aliased truncation introduced above (the proof is not detailed in this paper).

It is apparent from the proofs of these statements that for the violation of the Jacobi identity and the conservation laws the misrepresented interactions are responsible. Most of the misrepresented interactions are related to wavenumbers close to the truncation limit. Therefore, if the absolute value of the high-wavenumber spectral coefficients were small enough over the whole period of integration, the structure and the preservation of higher order Casimirs may be improved.

Take the aliasing-free truncation as an example. If all spectral coefficients associated with wavenumbers larger than T/2 are kept somehow zero then for $|\mathbf{k}| \leq T/2$ Eq. (12) is valid because the $\zeta_{\mathbf{e}_i}$-s of a nonzero N-fold product occur in all possible permutations in Eq. (13). On the other hand the components in the gradient of the Hamiltonian that are related to $|\mathbf{k}| > T/2$ are also zero. This guarantees the preservation of the Casimirs according to Eq. (7). Notice, however, that these invariants would not be Casimirs in the sense of Eq. (2), because their conservation were not independent of the particular form of the Hamiltonian. Unfortunately, however, the ideal fields with zero large wave-number coefficients cannot be maintained.

Since Liouville's theorem and ergodicity apply for these schemes, the time average of the spectral energy distribution can be estimated with the canonical equilibrium phase-space average as it was given by *Kraichnan* (1967). If the ratio of the average wavenumber $k^* = \sqrt{C^2/H}$ and the truncation wavenumber T is small enough, the energy spectrum has a maximum at large scales and declines towards the small scales proportionally to the reciprocal of the wavenumber (*Fox* and *Orszag*, 1973). Since the number of wave vectors in a wavenumber band increases linearly with increasing wavenumber, a significant amount of energy can remain on the small scale part of the spectrum in the canonical distribution. On the other hand, if the initial field is such that the energy is only on given scales and the cutoff wavenumber is large enough compared to these scales then it takes a while for the energy to flow to higher wavenumbers, and until this happens the large scale coefficients and their interaction will dominate. Thus for a flow dominated by a given scale the conservation of the structure and higher order Casimirs can be improved for a

finite-time interval by increasing the resolution. In this respect the advantage of using higher resolution numerical weather prediction models is not the enhanced representation of small scales but the improved control of the synoptic scale motions through better conservation of the invariants.

In numerical practice the favorable steep energy spectrum is also maintained by the introduction of scale-selective viscosity terms. These terms were originally applied to reduce the effects of "blocking errors" related to the nonrepresented interactions in the aliasing-free models (*Machenhauer*, 1991) and to eliminate the aliasing from the aliased schemes (*Orszag*, 1971). From our point of view, however, they can also help to improve the conservation of the structure in the inertial range. On the other hand, these viscosity terms constantly decrease the enstrophy indicating the destruction of the Casimir invariants. At the same time dissipation has only a slight effect on the conservation of energy, which leads to the decrease of k^*. The energy spectrum becomes steeper and steeper, thus the scale-selective dissipation can cause an increase at the large scale part of the energy spectrum. This is the "tail wagging the dog" effect described by e.g. *Frederiksen et al.* (1996). Long term integration of relevant atmospheric models have to account for dissipative processes anyway, but one must recall that the role of the viscosity and diffusion terms is in one part to simulate the realistic dissipation, in another to control the truncation errors. Consequently, traditional truncations can accurately simulate the conservative Hamiltonian nature of the inertial wavenumber range between the forced and dissipative scales, if the cut-off wavenumber is large enough and the initial data are properly processed.

4.3 Structure preserving truncation strategies

4.3.1 The sine-bracket equation

So far only one truncation of the vorticity equation has been shown to preserve the Hamiltonian structure of the equations, and there are strong indications that this may be a unique one (*Zeitlin*, 1991; *Dowker* and *Wolski*, 1992; *McLachlan*, 1993). This sine-bracket truncation first proposed by *Zeitlin* (1991) is named after the underlying algebraic structure that was first introduced by *Fairlie et al.* (1989) and *Fairlie* and *Zachos* (1989). The governing equation is a slight modification of the aliased truncation of Eq. (8),

$$\frac{d\zeta_{\mathbf{m}}}{dt} = \sum_{\substack{n_1,n_2=-T \\ \mathbf{n}\neq\mathbf{0}}}^{T} \frac{1}{\epsilon} \frac{\sin(\epsilon\,\mathbf{m}\times\mathbf{n})}{|\mathbf{n}|^2}\, \zeta_{\mathbf{m}+\mathbf{n} mod M}\, \zeta_{-\mathbf{n}}, \tag{17}$$

where $\epsilon = 2\pi/M$ and $M = 2T+1$. The entries of the structure matrix are

$$\mathbf{D}_{\mathbf{mn}} = \frac{1}{\epsilon} \sin(\epsilon\, \mathbf{m} \times \mathbf{n})\, \zeta_{\mathbf{m}+\mathbf{n} mod M}\,. \tag{18}$$

Due to the feature of the sine function the structure matrix is obviously skew-symmetric and the Jacobi identity also holds. Hence Eq. (17) is a Hamiltonian system.

Note that in the limit $\epsilon \to 0$ (as $T \to \infty$) the term in Eq. (17) associated with given $\mathbf{m}$ and $\mathbf{n}$ wave vectors will be identical with the corresponding term of Eq. (8). The value of $\epsilon \mathbf{m} \times \mathbf{n}$ in general, however, will not tend to zero with increasing resolution. The smoothness of the vorticity field, i.e. the fact that the spectral coefficients tend to zero as the wave vectors grow to infinity, would ensure the convergence of Eq. (17) to Eq. (8), (*Miller et al.*, 1992; *Hoppe*, 1989), but this ideal case cannot be maintained in an inviscid fluid (see previous section).

4.3.2 Invariants of the sine-bracket equation

The conservation of energy in the system Eq. (17) is a straightforward consequence of the skew-symmetry of the structure matrix. The most important new feature of the sine-bracket equation in contrast to the traditional truncations is that it preserves the Jacobi condition and possesses $2T$ independent Casimir invariants. Their general form is

$$C_s^N = \sum_{I^N} \zeta_{\mathbf{i}_1} \cdots \zeta_{\mathbf{i}_N} \cos\left(\epsilon\, 2A(\mathbf{i}_1,\ldots,\mathbf{i}_N)\right), \tag{19}$$

$$I^N = \{(\mathbf{i}_1,\ldots,\mathbf{i}_N),\ \sum_{j=1}^{N} \mathbf{i}_j = \mathbf{0} mod M\}, \tag{20}$$

where $2 \le N \le 2T$ and $A(\mathbf{i}_1,\ldots,\mathbf{i}_N)$ denotes the area spanned by the index vectors

$$A(\mathbf{i}_1,\ldots,\mathbf{i}_N) = \frac{1}{2}\left(\mathbf{i}_2 \times \mathbf{i}_1 + \mathbf{i}_3 \times (\mathbf{i}_1 + \mathbf{i}_2) + \ldots + \mathbf{i}_N \times (\mathbf{i}_1 + \ldots + \mathbf{i}_{N-1})\right). \tag{21}$$

(For proof see Appendix C.) Note that C_s^2 is the enstrophy.

Again, the cosine factor would tend to unit for a given index set if $T \to \infty$, but C_s^N will be identical with the Casimirs $\mathcal{C}^N$ of Eq. (8) for $2 < N \le 2T$ in the limit $T \to 0$ only if the vorticity field were smooth.

The impressive properties of structure conservation and of having an increasing number of invariants with increasing resolution suggest that the time

evolution of the sine-bracket system is controlled by an increasing number of natural constraints that should be important for the long-term model integrations. On the other hand it eliminates the structure-destroying effects of aliasings at the price of distorting the well represented interactions. Moreover, the invariants at low resolution substantially differ from the invariants of the original system Eq. (8), and in contrast to the quadratically growing number of dynamical variables the number of extra invariants increases only linearly with resolution. As the resolution increases Eq. (17) gives better and better approximation of Eq. (8) for the large scale part of the spectrum, but with suitably processed initial data it is also true for the traditional schemes. The theoretical considerations and numerical experiments of *Hattori* (1993) showed that the extra invariants of the sine-bracket truncation have only slight impact on the statistical mechanics of the finite-mode vorticity equation.

5. Truncation strategies to quasi-geostrophic layer models

It was shown in *McLachlan et al.* (1997) that the quasi-geostrophic layer models also have Hamiltonian structure and an infinite number of invariants. Albeit simple, these are important models of the atmosphere, because they are capable to simulate baroclinic instabilities even in case of only two layers and low resolution. Fortunately, similar truncation methods can be applied as to the two-dimensional vorticity equation, moreover, a slightly modified version of the same time integrator can be used for the numerical integrations. We briefly describe the model equations and invariants of the N-layer model, a more detailed description can be found in *Pedlosky* (1987) and *McLachlan et al.* (1997).

The N-layer quasi-geostrophic model consists of N linearly coupled layers with different but constant densities. The velocity field and the pressure field are connected through the geostrophic relation and the stream function is identified with the pressure. The continuous equations governing this system are

$$\frac{\partial q^{(i)}}{\partial t} = \partial(q^{(i)},\psi^{(i)}),\ i = 1,...,N, \tag{22}$$

where $\partial(f,g) = \frac{\partial f}{\partial x}\frac{\partial g}{\partial y} - \frac{\partial f}{\partial y}\frac{\partial g}{\partial x}$, and the potential vorticity $q^{(i)}$ and the stream function $\psi^{(i)}$ of the i-th layer ($i = 1,...,N$) are connected through

$$q^{(i)} = -D^{(i)}\{\nabla^2\psi^{(i)} - F^{(i)}\{(1-\delta_{iN})(\psi^{(i)} - \psi^{(i+1)}) + (1-\delta_{i1})(\psi^{(i)} - \psi^{(i-1)})\}\}. \tag{23}$$

Here $F^{(i)}=f^2L^2/D^{(i)}g(\Delta\rho/\rho_0)$, where f is the Coriolis parameter, g is the acceleration due to gravity, L is a characteristic horizontal scale, ρ_0 and $\Delta\rho$ are a characteristic value of the density and its variation between neighboring layers, respectively, and $D^{(i)}$ is the relative thickness of the i-th layer in the absence of motion $\left(\sum_{i=1}^{N} D^{(i)}=1\right)$. Note that assuming equal density jumps between neighboring layers $F^{(i)}D^{(i)}=F^{(j)}D^{(j)}$ for all $i,j\in\{1,\ldots,N\}$.

Transformed via two-dimensional Fourier transformation with periodic boundary conditions, the equivalent ordinary differential equations are

$$\dot{q}_{\mathbf{m}}^{(i)}=\sum_{\mathbf{n}}(\mathbf{m}\times\mathbf{n})\,q_{\mathbf{m}+\mathbf{n}}^{(i)}\,\psi_{-\mathbf{n}}^{(i)}, \tag{24}$$

where $\mathbf{m}\times\mathbf{n}=m_1n_2-m_2n_1$ and $q_{\mathbf{m}}^{(i)}$, $\psi_{\mathbf{m}}^{(i)}$ are the spectral coefficients of the i-th layer potential vorticity and stream function, respectively, associated with the wave vector $\mathbf{m}$.

The spectral transforms of the potential vorticity and the stream function are related by

$$\left(\psi_{\mathbf{n}}^{(1)},\ldots,\psi_{\mathbf{n}}^{(N)}\right)^T=\mathbf{B}_{\mathbf{n}}\left(q_{\mathbf{n}}^{(1)},\ldots,q_{\mathbf{n}}^{(N)}\right)^T\equiv\mathbf{B}_{\mathbf{n}}\mathbf{q}_{\mathbf{n}} \tag{25}$$

with $\mathbf{B}_{\mathbf{n}}$ being the inverse of the following symmetric tridiagonal matrix

$$\begin{bmatrix} D^{(1)}(n^2+F^{(1)}) & -\hat{F} & & & & & \\ -\hat{F} & D^{(2)}(n^2+2F^{(2)}) & -\hat{F} & & & & \\ & \ddots & \ddots & \ddots & & & \\ & & \ddots & \ddots & \ddots & & \\ & & & -\hat{F} & D^{(N-1)}(n^2+2F^{(N-1)}) & -\hat{F} & \\ & & & & -\hat{F} & D^{(N)}(n^2+F^{(N)}) & \end{bmatrix}, \tag{26}$$

where n^2 stands for $|\boldsymbol{n}|^2$ and $\hat{F}$ for $D^{(i)}F^{(i)}$. Since the Hamiltonian of this system is

$$H = \frac{1}{2} \sum_{\mathbf{n}} \mathbf{q}_{\mathbf{n}}^{T} \mathbf{B}_{\mathbf{n}} \mathbf{q}_{-\mathbf{n}}, \tag{27}$$

and $\mathbf{B}_{\mathbf{n}}$ is also symmetric,

$$\psi_{-\mathbf{n}}^{(i)} = \left(\nabla_{\mathbf{q}_{\mathbf{n}}} H\right)^{(i)}. \tag{28}$$

Thus Eq. (24) defines a Hamiltonian system for each layer with a corresponding structure matrix

$$\mathbf{D}_{\mathbf{mn}}^{(i)} = (\mathbf{m} \times \mathbf{n})\, \mathbf{q}_{\mathbf{m}+\mathbf{n}}^{(i)}. \tag{29}$$

In this model the potential vorticity of each layer is an individually conserved quantity, thus the integrals of any functions of the potential vorticity give the integrals of motion. The Casimir invariants of the system with spectral coefficients read

$$Q^{(i)k} = \sum_{I^k} q_{\mathbf{i}_1}^{(i)} \cdots q_{\mathbf{i}_k}^{(i)}, \quad (i = 1,\ldots,N), \tag{30}$$

$$I^k = \{(\mathbf{i}_1,\ldots,\mathbf{i}_k) \,|\, \sum_{j=1}^{k} \mathbf{i}_j = \mathbf{0}\}. \tag{31}$$

As it is described in *McLachlan et al.* (1997) for the two-layer system, there exists a similar structure-preserving truncation to the N-layer model as to the two-dimensional vorticity equation:

$$\dot{q}_{\mathbf{m}}^{(i)} = \sum_{\mathbf{n} \in \mathbf{I}} (1/\epsilon) \sin(\epsilon\, \mathbf{m} \times \mathbf{n})\, q_{\mathbf{m}+\mathbf{n}}^{(i)} (\mathbf{B}_{-\mathbf{n}} \mathbf{q}_{-\mathbf{n}})^{(i)}, \tag{32}$$

where $\epsilon = 2\pi/M$, and the index set is defined by

$$\mathbf{I} = \{\mathbf{i} \in \mathbf{Z}^2 \,|\, -T \le i_1, i_2 \le T,\ \mathbf{i} \neq \mathbf{0},\ T = (M-1)/2\}. \tag{33}$$

The finite dimensional system obtained with the above truncation is Hamiltonian, and possesses $N \cdot 2T$ integrals of motion, but again the Casimirs of this system $Q_s^{(i)k}$ for $k > 2$ converge to the Casimirs of the original system in the limit $T \to \infty$ only if the potential vorticity fields are smooth. The Casimirs are

$$Q_s^{(i)k} = \sum_{\mathbf{I}^k} q_{\mathbf{i}_1}^{(i)} \cdots q_{\mathbf{i}_k}^{(i)} \cos[\epsilon\,(2A(\mathbf{i}_1,\ldots,\mathbf{i}_k))], \quad (i = 1,\ldots,N), \tag{34}$$

$$\mathbf{I}^k = \{(\mathbf{i}_1,\ldots,\mathbf{i}_k) \,|\, \sum_{j=1}^{k} \mathbf{i}_j = \mathbf{0} \, mod M\}, \tag{35}$$

where $2 \leq k \leq 2T$ and $A(\mathbf{i}_1,\ldots,\mathbf{i}_k)$ is given in Eq. (21).

In order to be able to extend our comparative study to the hierarchy of quasi-geostrophic layer models, we consider also a truncation that is the counterpart of the traditional truncation applied to the two-dimensional vorticity equation: retaining the same set of coefficients as in Eq. (32), the index $(\mathbf{m}+\mathbf{n}) mod M$ is used instead of $\mathbf{m}+\mathbf{n}$ and the coefficients of the nonlinear terms are modified to $(\mathbf{m}\times\mathbf{n}) mod M$ if $|m_1+n_1|>T$ or $|m_2+n_2|>T$. This truncation destroys the Hamiltonian structure, but ensures the conservation of energy and potential enstrophy.

6. Numerical experiments

6.1 Algorithm for integration

Numerical experiments were carried out in order to compare the time-depending characteristics of the structure preserving and of the traditionally truncated systems described in Section 4 and 5. One can argue that a fair comparison between the traditional and the structure preserving schemes should involve the aliasing-free traditional scheme, which is assumed to be superior to the aliased truncation of this study. The superiority of the aliasing-free schemes in the numerical practice, however, is not obvious since (1) the finite-difference models, though inevitably burdened by aliasing, proved to be competitive with the aliasing-free spectral schemes, moreover (2) there are numerical evidences that the aliased spectral schemes may perform even better than the aliasing-free methods (*Chen*, 1997).

A slightly modified version of McLachlan's explicit scheme (*McLachlan*, 1993) was used in our experiments for the integration of the two-dimensional vorticity equation (hereafter denoted by 2DV). It will be indicated in the descriptions of the experiments whether the first or the second order version of the time integrator was used. *McLachlan et al.* (1997) describes, that with some modification the integration algorithm used for the integration of the two-dimensional vorticity equation can be used for the structure preserving truncation of the quasi-geostrophic equation. We carried out experiments with the two-layer quasi-geostrophic model (hereafter denoted by L2 QG). For details of the

integration scheme see Appendix of Part I and *McLachlan et al.* (1997). The main advantages of this algorithm are its efficiency and the fact that it can be applied to the traditionally truncated aliased systems as well. This makes possible a fair comparison between the traditional and the structure preserving schemes even in extremely long term integrations.

6.2 Verification of the conservation properties

6.2.1 Conservation of the energy

Energy cannot be an exact invariant of the discrete Hamiltonian system even if the time stepping algorithm is symplectic. There is, however, a modified Hamiltonian in this case which is conserved and this ensures the boundedness of the energy error, in addition, the perturbation in the value of the Hamiltonian can be reduced to arbitrary small value with higher and higher order schemes (see Part I). Although the traditional spatial truncation conserves formally the energy and the enstrophy, the boundedness of energy errors over the time integration is not guaranteed. Possibly the fewer constraints exerted by the fewer formal invariants allow greater errors of energy. To investigate whether this conjecture is true, we calculated the relative energy error, $(H(t)-H(0))/H(0)$, and compared the results obtained with the differently truncated systems.

The models were integrated from randomly generated initial fields for 10^6 time steps at resolutions T1 and T2, and for 10^5 time steps at T13. The time step was uniformly set to 1.0 and the second order time integration scheme was used. Care should be taken when the results at the given resolutions are compared, because the uniform time step has different meaning for the different size systems. If the reciprocal of the average (potential-)vorticity $1/\bar{\zeta}$ is taken as a characteristic time unit, then the unit time step corresponds to $\bar{\zeta}$ nondimensional time units. Since a similarly defined characteristic time unit for the atmosphere is 10^5 sec, an atmospheric equivalent time step for the unit time step in the different size systems can be obtained by taking $\bar{\zeta} \times 10^5$ sec. The initial average vorticity was 0.09796 1/sec, 0.06091 1/sec and 0.00801 1/sec at T1, T2 and T13, respectively, in the 2DV model, while the average potential vorticity in the L2 QG model runs were of the magnitude 10^{-2} 1/sec at all three resolutions. With these initial fields, an equivalent atmospheric time step of 160 min., 102 min. and 13 min. can be attributed to the discretized systems at T1, T2 and T13 in case of the 2DV model and a time step of about 15 min. to the L2 QG model at all three resolutions.

Fig. 1 shows the relative energy errors for the structure preserving and the traditional truncation at T2 and T13. The result for the structure-preserving truncation of the model at T1 can be seen in Fig. 4a of Part I. At T1 the magnitudes of the relative errors obtained with the traditional truncation are the same (not shown), which can be the consequence of the fact that at T1 even the

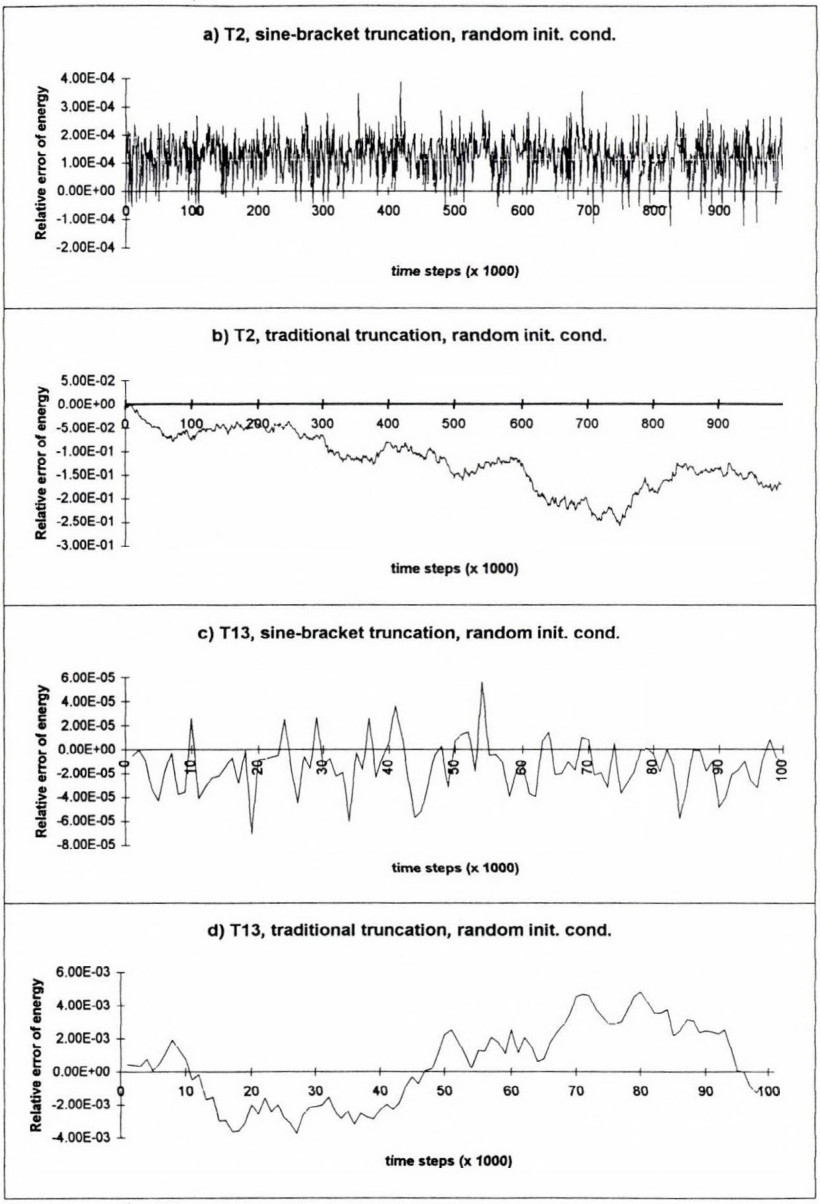

Fig. 1. Relative error of energy over a 10^6 time-step integration of the 2DV model at T2 started from randomly generated initial condition integrated with (*a*) the structure-preserving scheme, (*b*) the traditional scheme; relative error of energy over a 10^5 time-step integration of the 2DV model at T13 started from randomly generated initial condition integrated with (*c*) the structure-preserving scheme, (*d*) the traditional scheme.

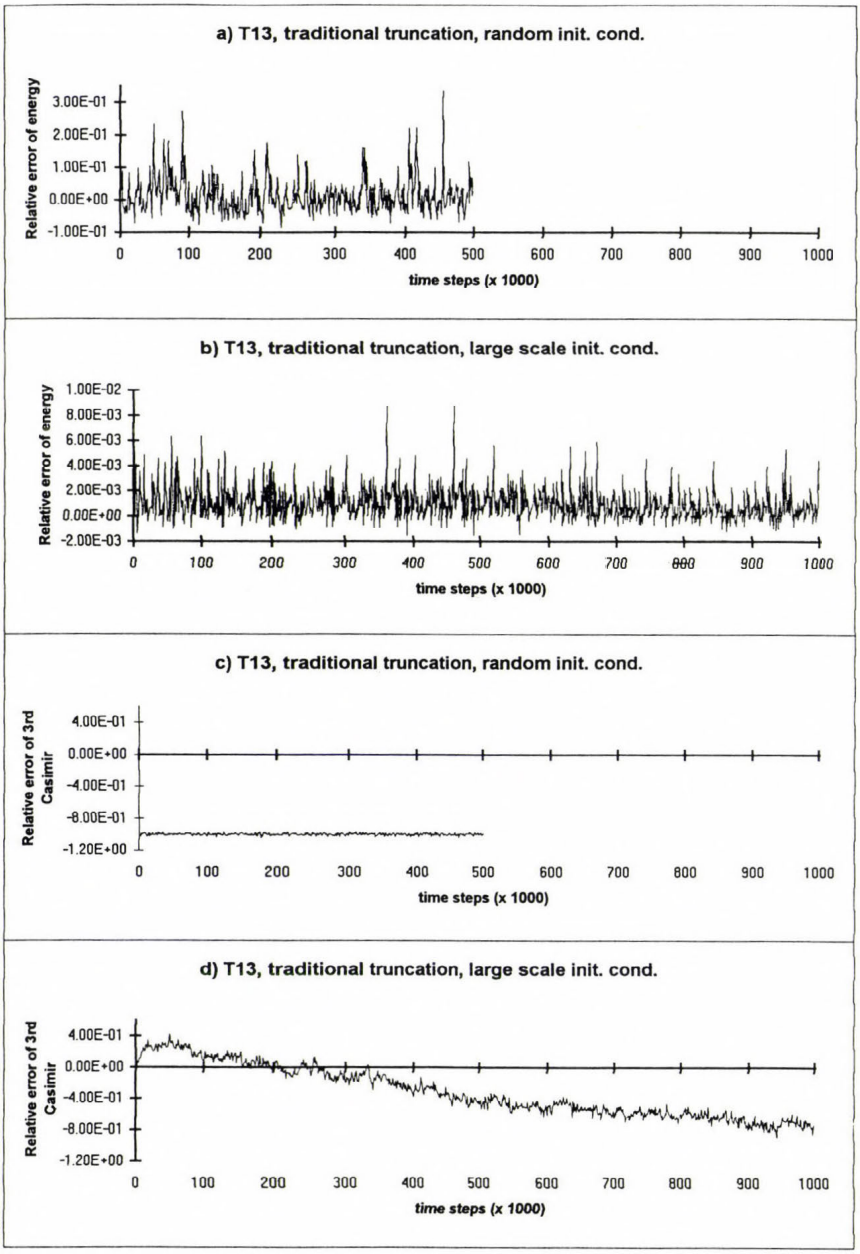

Fig. 2. Relative error of the energy and of the 3-rd Casimir (C^3) over a 5×10^5 time-step integration of the 2DV model at T13 integrated with the traditional scheme started from (*a*), (*c*) randomly generated initial condition, (*b*), (*d*) large scale ($|\boldsymbol{k}| \leq 3$) initial condition.

aliased truncation is Hamiltonian. Actually, the distinction "structure preserving" vs. "traditional" are not very useful in case of the maximum truncation, since it does not reflect the algebraic structure of the schemes. At T1 the relative errors oscillate around a nonzero value but do not exhibit any increasing tendency. At T2 there are profound differences between the performances of the schemes (see Fig. 1a, b). The error bound is three orders of magnitude larger and the relative error seems to have an increasing trend for the traditional scheme. The behavior of the structure conserving model is very similar to that of the T1 case. The difference is similar at T3, and T4 (not shown) but is somewhat less pronounced at T13 (Fig. 1c, d), especially with other initial conditions (see below the rotating cone experiment). At T13 the relative errors are oscillating around a nonzero value even in the traditionally truncated system. The relative energy curves obtained with the L2 QG model are not shown, since similar statements can be made about them as for the 2DV model runs.

It is not surprising that the truncation affects the results less at higher resolutions: a linearly growing number of constraints cannot control the evolution of a system with quadratically growing number of degrees of freedom. On the other hand, the constraints of statistical physics on the energy spectra can act only at higher resolution. Because of the validity of Liouville's theorem these constraints are present in both systems. As it was indicated in Section 4.2.4 until the ratio of the average and the cut-off wavenumber is small and the energy spectrum is steep enough toward small scales, an improvement in the preservation of structure in the traditional schemes can be achieved. This idea was tested by confining the energy in the initial condition to the large ($|\mathbf{k}| \leq 3$) scales at T13 (*Fig. 2a, b*). As expected, the energy error in the traditional system is two orders of magnitude smaller than for random initial conditions. It suggests that the effect of misrepresented interactions are less pronounced. On the other hand, similar improvement can be seen for the sine-bracket truncation due to the reduction of the role of the ill-represented interactions between the high wavenumbers. One must not forget, however, that the reduced errors of the time integration scheme for smoother fields can also contribute to the improvement of the results.

6.2.2 Conservation of the Casimir invariants

The conservation of Casimir invariants can also be characterized by their relative errors. The most important Casimir, the enstrophy (C^2) is not only a formal invariant, but it is a very effective numerical constraint for both truncation strategies. The error of the enstrophy over a time step is approximately equal to the expectation of the roundoff error for both models.

The higher order invariants, C_s^N-s of the sine-bracket model were computed from $N=3$ up to $N=2T$ for the different resolutions. The results of T2 are shown in *Fig. 3*. Due to the fact that these quantities are conserved within the roundoff error over a time step, they also impose strong constraints on the model variables. Note that the high accuracy of the Casimirs was found independent of the model resolution and of the order of the invariants. The special role of Casimir invariants in long-term numerical integration is based on this fact: the conservation of the Casimir invariants is independent of the systematic errors that occur in the model variables. The Casimirs remain independent integration constraints for any time. That is why the purely enstrophy preserving schemes have a better performance in the effective conservation of energy than those ensuring the formal invariance of only energy (see. e.g. *Sadourny*, 1975).

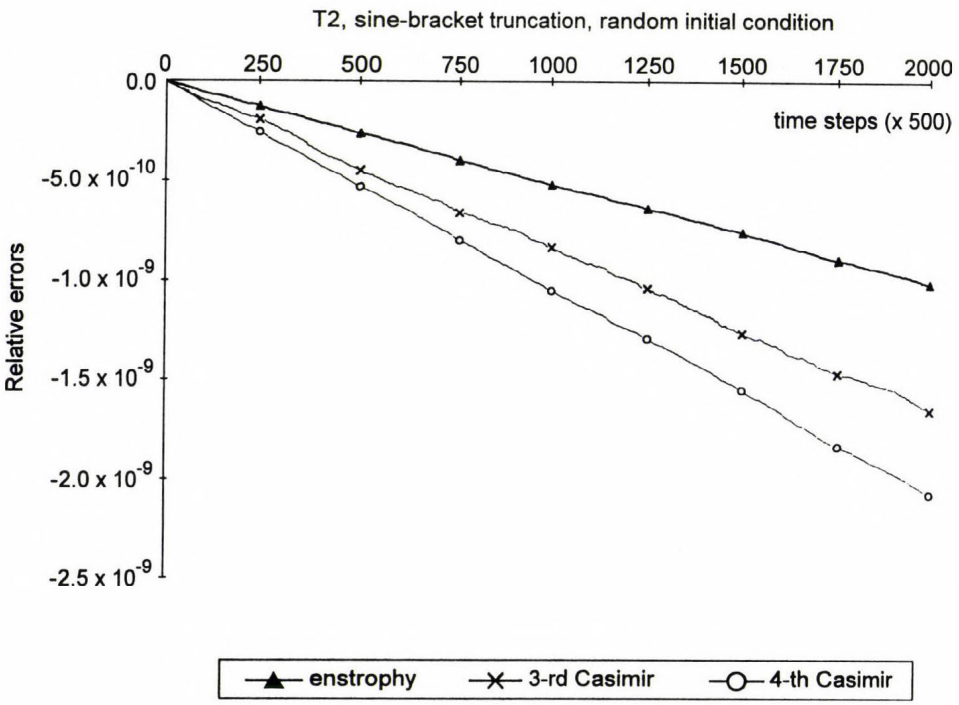

Fig. 3. Relative error of the first three Casimir invariants in the sine-bracket truncation of the 2DV model at T2. The initial condition was randomly generated, the integration was carried out for 10^6 time steps.

The smaller relative energy error for large scale initial fields can be attributed in parts to the smoothness of the vorticity field, thus it does not necessarily prove better structure conservation. A more appropriate indicator of the improvement in the preservation of structure is the relative error in the higher order Casimirs, which are not formal invariants in the traditional truncated system. *Fig. 2c, d* present the relative error of the finite analogue of Casimir $\mathcal{C}^3$ versus time for different initial conditions at T13. Started from random initial conditions the relative errors oscillate around a 100 percent right from the beginning. When the large scale random initial conditions are applied the maximum relative error is only about 40 percent during the first part of the integration. This indicates that there is indeed an improvement, though not substantial, in the preservation of structure in the traditional scheme for suitable initial conditions.

Another way of verifying conservation properties of a truncated system is to investigate the behavior of the discrete analogues of the continuous Casimir invariants in the physical space. As in *Hattori* (1993), we transformed back the spectral coefficients of vorticity to the physical space, then calculated the flatness (F) and skewness (S) parameters that are combinations of discrete analogues of continuous invariants (of $\mathcal{C}^4$, $\mathcal{C}^3$ and $\mathcal{C}^2$). Their definitions are the followings:

$$F = M^2 \frac{\sum_{\mathbf{k}\in\Omega} \zeta^4(\mathbf{k})}{\left[\sum_{\mathbf{k}\in\Omega} \zeta^2(\mathbf{k})\right]^2}, \qquad S = M \frac{\sum_{\mathbf{k}\in\Omega} \zeta^3(\mathbf{k})}{\left[\sum_{\mathbf{k}\in\Omega} \zeta^2(\mathbf{k})\right]^{3/2}}, \tag{36}$$

where $\zeta(\mathbf{k})$ denotes the vorticity at a grid point indexed by $\mathbf{k}$ of the lattice $\Omega = \{\mathbf{k} \mid -T \le k_1, k_2 \le T,\ T = (M-1)/2\}$. These quantities are frequently used to characterize vorticity distributions in a statistical sense. In our approach they can be viewed as discrete approximations to quantities that are individually conserved in the continuous case. (Note that the denominator is the power of enstrophy, which is conserved even in the truncated systems to a high degree of precision). We calculated the values of these parameters for different initial conditions in the two differently truncated systems. The results for the 2DV model at T13 are summarized in *Fig. 4*.

One apparent common feature on the panels is that the individual conservation laws are violated in all cases. Although the structure preserving schemes conserves their Casimirs accurately, these invariant quantities differ from the discrete analogues of the Casimirs of the original system, and their preservation does not guarantee the conservation of the latters.

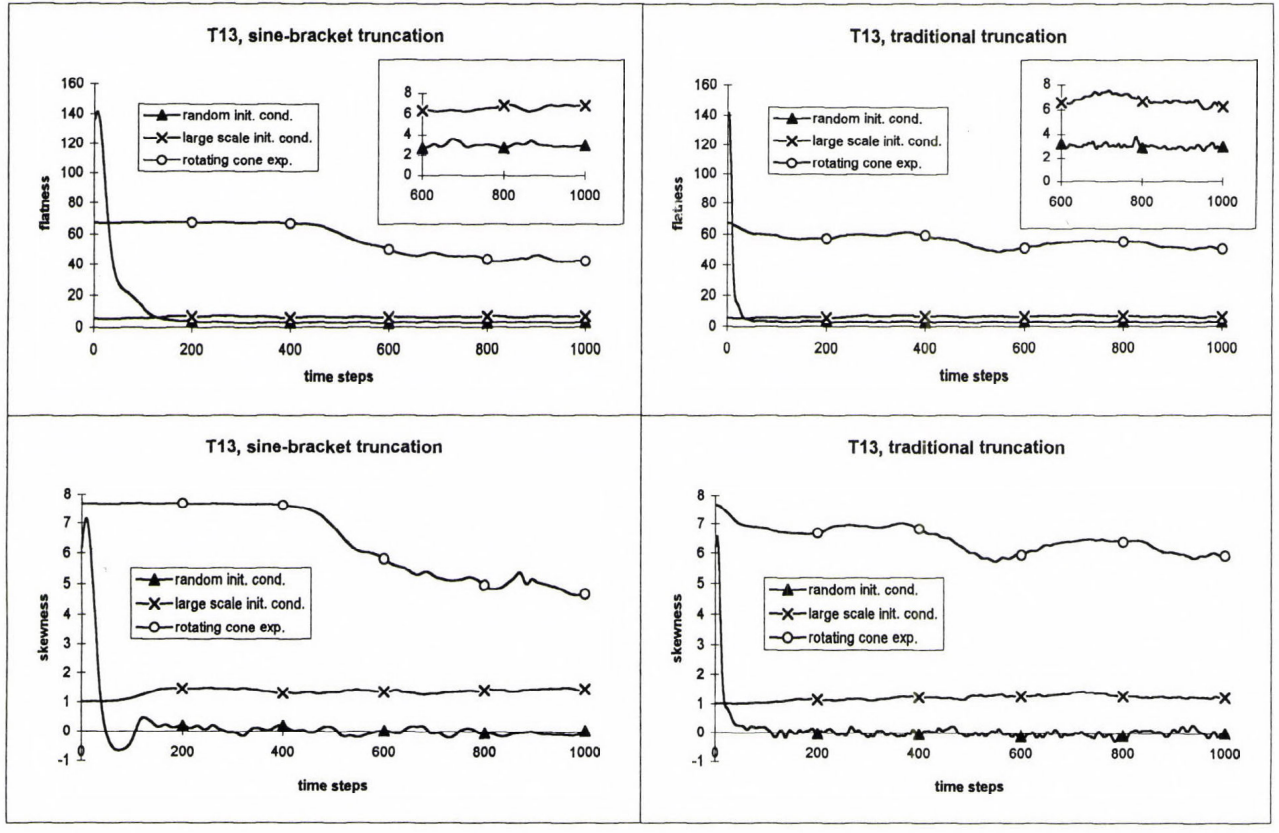

Fig. 4. Flatness and skewness (Eq. (36)) parameters in the 2DV model truncated with the traditional and the sine-bracket truncation at T13 integrated from different initial conditions (indicated on the curves) for 10^3 time steps.

When the initial fields are randomly generated the value of the parameters tend to those characterizing normal distribution ($F=3.0$ and $S=0.0$) in both truncated systems. The evolution of vorticity distribution, however, seems to be highly dependent on the initial condition — at least on the time scale represented by 10^3 time steps. In case of large scale initial field or in the rotating cone experiment (described below), the investigated statistical parameters are far from that of a normal distribution. There are differences in details, but the behavior of the two schemes in case of large scale initial condition is qualitatively similar. In both system the distribution is broader than the normal ($F \geq 3.0$) and less symmetric ($S \geq 0.0$, i.e skewed to the right).

In the third experiment the initial field was the discrete approximation of the vorticity field defined as

$$\zeta(\mathbf{r},t=0) = \begin{cases} 1 - \dfrac{|\mathbf{r}|}{r_0} & \text{for } |\mathbf{r}| \leq r_0 \\ 0 & \text{for } |\mathbf{r}| > r_0 \end{cases}, \tag{37}$$

where r_{01}, r_{02} are fixed numbers ($r_{01}=3$ and $r_{02}=7$ were used in the calculations at T13) and $\mathbf{r}=(r_1,r_2)$, $|\mathbf{r}| = \left((r_1-r_{01})^2+(r_2-r_{02})^2\right)^{\frac{1}{2}}$ and $r_0=(r_{01}^2+r_{02}^2)^{\frac{1}{2}}$. Visually, this field is a cone rotating around an axis at $\mathbf{r_0}=(r_{01},r_{02})$. The corresponding stream function field is

$$\psi(\mathbf{r},0) = \begin{cases} \dfrac{1}{4}|\mathbf{r}|^2 - \dfrac{1}{9r_0}|\mathbf{r}|^3 & \text{for } |\mathbf{r}| \leq r_0 \\ 0 & \text{for } |\mathbf{r}| > r_0 \end{cases}. \tag{38}$$

The latter can be written in the form

$$\psi(\mathbf{r},0) = \sum_{i=0}^{3} a_i \zeta^i(\mathbf{r},0) = \sum_{i=0}^{3} \frac{a_i}{i+1} \nabla_\zeta \mathcal{C}^{i+1}, \tag{39}$$

that is, this initial condition defines a steady state solution of the continuous vorticity equation which is constrained by the first four Casimir invariants (see Eq. (3)).

With this initial condition both statistical parameters have much larger values. An interesting fact, that the sine-bracket truncation succeeds in

preserving the initial value of the parameters up to about 400 time steps with this initial condition.

The cone defined in Eq. (37) is a steady solution of the continuous equation, and the initial fields are inevitably burdened with truncation errors. Unfortunately, the stability of this steady solution cannot be determined with the criteria given by Arnold for the nonlinear (Liapunov-)stability of the flow (see *Arnold*, 1989, 335 pp). Keeping in mind that the eventual breaking down of the initial vorticity pattern can be the result of the instabilities inherent in the initial conditions, we use this initial field for comparing the performance of the different schemes in terms of the effective conservation of the first four invariants and the accuracy of the individual variables. It can be expected, that if the conservation of the first four invariants in the two schemes differ substantially, the computed states in the two systems will also diverge. Since the results are affected by high truncation errors in the numerical integration, the comparative experiments were carried out at different high resolutions with the first order scheme. The cone was defined in the physical space and the spectral coefficients were computed via Fourier interpolation at a spectral truncation T13, T40, and T62. The model was integrated for 2×10^5 time steps at T13. The time evolution of the fields is shown in *Fig. 5a, c* and *Fig. 5b, d* for the structure preserving and the traditional scheme, respectively. On the base of the results neither of the schemes can be judged superior to the other. After some initial jumping the energy of both systems oscillate around an energy level about 3 percent lower than the initial level (not shown). The magnitude of energy fluctuations in the traditional model is roughly half of that in the structure conserving one. The cone completely disappears by the end of the integration. The T40 and T62 versions of both models were integrated for 5×10^3 time steps. In these experiments a cone of the same size was situated at the same part of the field as in the T13 case. *Fig. 5e-l* show the resulting vorticity and vorticity error fields at the final time. On the one hand the improvement of the results with increasing resolution is obvious, on the other the difference between the two models is hardly noticeable. The error fields in the sine-bracket model are a bit smoother and have slightly smaller extrema.

7. Summary and discussion

In this paper the effect of spatial truncation on the Eulerian atmospheric model equations was examined. We pointed out that traditional strategies inevitably violate the Jacobi identity, thus destroy the underlying Hamiltonian structure of the untruncated equations. At the same time these truncation methods necessarily ruin the preservation of nonquadratic Casimir invariants. As it was shown in Section 4 both the Jacobi identity and the conservation of Casimirs fail because of the misinterpreted interactions between wavemodes whose structure

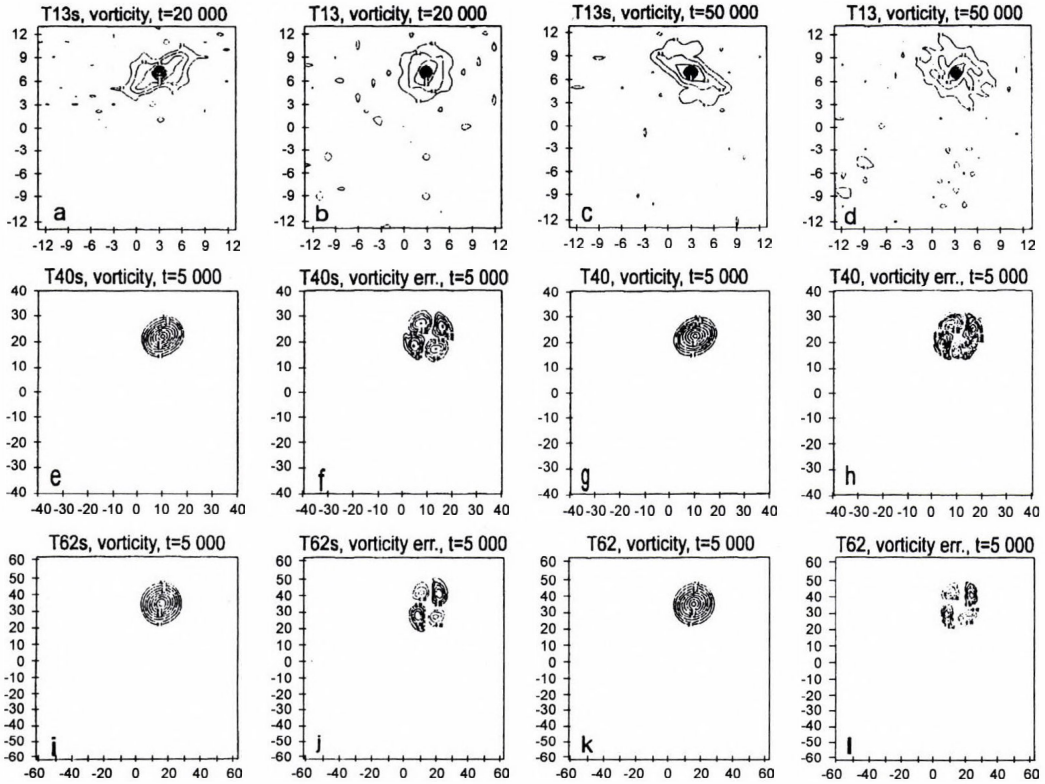

Fig. 5. Vorticity in the physical space in the rotating cone (Eq. 36) experiment (*a–d*) at T13, (*e–f*) at T40 and (*i–l*) at T62. Panels (*a*) and (*b*) show the vorticity field after $2\text{x}10^4$ time steps, while (*c*) and (*d*) correspond to the $5\text{x}10^4$-th time step in the structure-preserving and the traditional truncation, respectively. Panels (*e*), (*f*) and (*g*), (*h*) present the vorticity field and its error after $5\text{x}10^3$ time steps in the structure preserving and the traditionally truncated system, respectively, at T40. (*i*), (*j*) and (*k*), (*l*) is the same at T62.

function is distorted by the truncation. The number of misrepresented interactions is the largest for wavemodes that have a component close to the upper cutoff wavenumber. Consequently, an improvement in the conservation of the Hamiltonian structure can be achieved by reducing the role of the falsely represented interactions. This requires that the energy of the higher-wavenumber modes should be kept at a relatively low level. At this point an analogy between the higher-wavenumber modes and free gravity wave modes of the primitive equation models can be drawn. In both cases the problem can be handled by processing appropriately the initial data and continuously dissipating the energy of the problematic modes. On the other hand, the analogue of the filtered models is the structure preserving sine-bracket equation. The price for the preservation of structure and conservation of more invariants, however, must be paid: the sine-bracket equation is not aliasing-free, the high wavenumber interactions are distorted, and the higher order invariants ($N > 2$) converge to the Casimirs of the untruncated system only in the limit $T \to \infty$ and if the vorticity field is smooth. Operational and research models of today follow the first strategy using higher and higher cutoff wavenumbers and scale selective viscosity and diffusion terms. The small scale structure of such models, however, should be handled very carefully because the interactions associated with them are not constrained by higher order vorticity-type invariants. This fact might contribute to the highly unstable evolution of perturbations initially dominated by small scale structures (*Hartmann et al.*, 1995). The problem whether structure preserving schemes offer a better handling of these deficiencies can be investigated only on the base of extensive numerical experiments.

Another important aspect for the operational practice is the computational efficiency of the schemes. Executing all operations in the spectral space is supposed to have two main disadvantages: the high cost of evaluating the nonlinear terms and the difficulty to calculate some of the physical parameterization (see e.g. *Haltiner* and *Williams*, 1980). Although McLachlan's algorithm keeps the whole computational procedure in the spectral space, it reduces, though does not eliminate, the first problem to solving an equivalent diagonal system of linear equations. An additional advantage of this algorithm is that it can be even more efficient in a parallel computational environment. While it cannot be foreseen whether similar efficient algorithms can be developed for more sophisticated systems and how the problem of physical parameterization can be handled for these schemes, this method demonstrates that the utilization of hidden symmetries in the equations may result in a substantial improvement of the computational efficiency.

For theory oriented studies focusing on the phase space geometry, however, the algebraic structure preserving schemes are rather appealing. For instance, the Hamiltonian structure of the five-component Lorenz' model proved to have a crucial role in the precise definition of the slowest invariant manifold (*Bokhove* and *Shepherd*, 1996). This study, nonetheless, made use of the fact

that the maximum truncation traditional scheme, a real vorticity-triad, has Hamiltonian structure. As we stated in the main body of this paper for $T \geq 2$ there is no traditional truncated scheme, which retains the algebraic structure.

Finally, let us mention that while this study focused on the truncation of the Eulerian atmospheric equations there is another approach, the truncation of the Lagrangian equations themselves. There seems to be three different ways to realize this program: (1) application of the sine-bracket truncation to the Lagrangian equations (*Rouhi* and *Abarbanel*, 1993), (2) discretization of the action principle (*Holm et al.*, 1985) and (3) geometric models based on the semi-geostrophic approach (*Purser*, 1997 and references therein). Notice, however, that while the first two approaches have the appealing feature of preserving the structure, they destroy the particle relabelling symmetries and the related conservation laws. The most promising approach retaining the particle relabelling symmetries and the individual conservation laws is based on the semi-geostrophic equations. Opponents of this approach argue that (1) in contrast to the geostrophic equations the semi-geostrophic equations cannot be derived from the primitive equations by a formal expansion with respect to a small parameter as the Rossby number and (2) the semi-geostrophic equations are singular at the equator. Neither is an obstacle to applying this approach to a series of dynamical meteorological problems for which the Lagrangian approach is more relevant (e.g. for simulating the development of a frontal zone).

Acknowledgements—This work was partly supported by a grant from State Scientific Research Fund (OTKA F 019268). Encouraged by the informal discussions great progress was achieved during the authors' stay at the Isaac Newton Institute for Mathematical Sciences, Cambridge, England, within the program "Mathematics of the Atmosphere and Ocean Dynamics" in the summer and autumn of 1996.

References

Arakawa, A. and *Lamb, V.R.*, 1980: A Potential Enstrophy and Energy Conserving Scheme for the Shallow Water Equations. *Mon. Wea. Rev. 109*, 18-36.

Arakawa, A., 1966: Computational design for long-term numerical integration of equations of fluid of motions: Two-dimensional incompressible flow. Part I. *J. Comput. Phys. 1*, 119-143.

Arnold, V.I., 1989: *Mathematical Methods in Classical Mechanics*. Springer-Verlag, New-York, 508 pp.

Bennett, A.F. and *Middleton, J.F.*, 1983: Statistical mechanics of a finite-difference approximation to the barotropic vorticity equation. *Quart. J. Roy. Meteorol. Soc. 109*, 795-808.

Bokhove, O. and *Shepherd, T.*, 1996: On Hamiltonian balanced dynamics and the slowest invariant manifold. *J. Atmos. Sci. 53*, 276-297.

Chen, X.S., 1997: Use of the aliased spectral model in numerical weather prediction. *Mon. Wea. Rev. 125*, 2998-3007.

Dowker, J.S. and *Wolski, A.*, 1992: Finite model of two-dimensional ideal hydrodynamics. *Phys. Rev. A 46*, 6417-6430.

Fairlie, D.B., *Fletcher, P.* and *Zachos, C.K.*, 1989: Trigonometric structure constants for new infinite-dimensional algebras. *Phys. Lett. B. 218*, 203-206.

Fairlie, D.B. and *Zachos, C.K.*, 1989: Infinite-dimensional algebras, sine-brackets, and SU(∞), *Phys. Lett. B 224*, 101-107.

Fox, D.G. and *Orszag, S.A.*, 1973: Inviscid dynamics of two-dimensional turbulence, *Phys. Fluid. 16*, 169-171.

Frederiksen, J.S., *Dix, M.R.* and *Kepert, S.M.*, 1996: Systematic energy errors and the tendency toward canonical equilibrium in atmospheric circulation models. *J. Atmos. Sci. 53*, 887-904.

Haltiner, G.J. and *Williams, R.T.*, 1980: *Numerical Prediction and Dynamic Meteorology*. J. Wiley, New York, 477 pp.

Hartmann, D.L., *Buizza, R.* and *Palmer, T.N.*, 1995: Singular vectors: The effect of spatial scale on linear growth of disturbances. *J. Atmos. Sci. 52*, 3885-3894.

Hattori, Y., 1993: Effect of phase dependent invariants and ergodicity in finite-mode systems closely related with two-dimensional ideal flow. *J. Phys. Soc. Japan 62*, 2293-2305.

Holm, D.D., *Kupershmidt, B.A.* and *Levermore, C.D.*, 1985: Hamiltonian differencing of fluid dynamics. *Adv. Appl. Math. 6*, 52-84.

Hoppe, J., 1989: Diffeomorphism groups, quantization, and SU(∞). *Int. Journ. Mod. Phys. A 19*, 5235.

Kádár, B., *Szunyogh, I.* and *Dévényi, D.*, 1998: On the origin of model errors. Part I: Effects of the temporal discretization for Hamiltonian systems. *Időjárás 102*, 19-41.

Kraichnan, R.H., 1967: Inertial ranges in two-dimensional turbulence. *Phys. Fluid. 10*, 1417-1423.

Lorenz, E.N., 1960: Maximum simplification of dynamic equations. *Quart. J. Roy. Meteor. Soc. 12*, 243-254.

Machenhauer, B., 1991: Spectral methods. *Proceedings of ECMWF seminars on "Numerical methods in atmospheric models"*. Sept 9-13, Reading, UK. *Vol. 1*, 3-85.

McLachlan, R., 1993: Explicit Lie-Poisson integration and the Euler equations. *Phys. Rev. Lett. 71*, 3043-3046.

McLachlan, R.I., *Szunyogh, I.* and *Zeitlin, V.*, 1997: Hamiltonian finite-dimensional models of baroclinic instability. *Phys. Lett. 229A*, 299-305.

Miller J., *P. B. Weichman* and *M. C. Cross*, 1992: Statistical mechanics, Euler's equation, and Jupiter's Red Spot. *Phys. Rev. A*, *45*, 2328-2359.

Morrison, P.J., 1981: Hamiltonian field description of two-dimensional vortex fluids and guiding center plasmas. *PPPL-1783*, Princeton University, Princeton, New Jersey.

Olver, P.J., 1989: *Applications of Lie Groups to Differential Equations*. Springer-Verlag, 513 pp.

Orszag, S.A., 1971: On the elimination of aliasing in finite-difference schemes by filtering high-wavenumber components. *J. Atmos. Sci. 28*, 1074.

Pedlosky, J., 1987: *Geophysical Fluid Dynamics*. Second edition, Springer, New York, 710 pp.

Purser, R.J., 1997: Legendre-transformable semi-geostrophic theories. *J. Atmos. Sci.* (under review).

Rouhi, A. and *Abarbanel, H.D.I.*, 1993: Symmetric truncations of the shallow-water equations. *Phys. Rev. E*, *48*, 3643-3655.

Sadourny, R., 1975: The dynamics of finite-difference models of the shallow-water equations. *J. Atmos. Sci. 32*, 680-689.

Salmon, R. and *Talley, L.D.*, 1989: Generalization of Arakawa's Jacobian. *J. Comput. Phys. 83*, 247-259.

Shepherd, T.G., 1990: Symmetries, conservation laws, and Hamiltonian structure in geophysical fluid dynamics. *Adv. Geophys. 32*, 287-337.

Szunyogh, I., 1993: Finite-dimensional quasi-Hamiltonian structure in simple model equations. *Meteorol. Atmos. Phys. 52*, 49-57.

Zeitlin, V., 1991: Finite-mode analogs of 2D ideal hydrodynamics: Coadjoint orbits and local canonical structure. *Physica D 49*, 353-362.

Zeitlin, V. and *Pasmanter, R.A.*, 1994: On the differential geometry approach to geophysical flows. *Phys. Lett. A*, *189*, 59-63.

Appendix A

Proofs of statements in Section 4.2. The fact that an aliasing-free truncated system in general is not Hamiltonian follows from the lemma below:

Lemma: *Let a subsystem of the aliasing-free truncated system consist of the variables corresponding to the wave vectors* $\mathbf{i}, \mathbf{j}, \mathbf{k}, -\mathbf{i}, -\mathbf{j}, -\mathbf{k}$ *satisfying the conditions* $\mathbf{i}+\mathbf{j}=\mathbf{k}$ *and* $\mathbf{i}\times\mathbf{j}\neq 0$. *This subsystem, hereafter referred to as a vorticity-triad, possesses the following properties:*

(*i*) *It is Hamiltonian if and only if the spectral coefficients are real.*

(*ii*) *It conserves the energy and the enstrophy.*

Proof: The structure matrix for the vorticity-triad subsystem is

$$
\begin{array}{c}
\\
\mathbf{i} \\
\mathbf{j} \\
\mathbf{k} \\
-\mathbf{i} \\
-\mathbf{j} \\
-\mathbf{k}
\end{array}
\begin{array}{c}
\begin{array}{cccccc} \mathbf{i} & \mathbf{j} & \mathbf{k} & -\mathbf{i} & -\mathbf{j} & -\mathbf{k} \end{array} \\
\left[\begin{array}{cccccc}
0 & (\mathbf{i}\times\mathbf{j})\zeta_{\mathbf{k}} & 0^* & 0 & 0^* & (\mathbf{j}\times\mathbf{i})\zeta_{-\mathbf{j}} \\
(\mathbf{j}\times\mathbf{i})\zeta_{\mathbf{k}} & 0 & 0^* & 0^* & 0 & (\mathbf{i}\times\mathbf{j})\zeta_{-\mathbf{i}} \\
0^* & 0^* & 0 & (\mathbf{i}\times\mathbf{j})\zeta_{\mathbf{j}} & (\mathbf{j}\times\mathbf{i})\zeta_{\mathbf{i}} & 0 \\
0 & 0^* & (\mathbf{j}\times\mathbf{i})\zeta_{\mathbf{j}} & 0 & (\mathbf{i}\times\mathbf{j})\zeta_{-\mathbf{k}} & 0^* \\
0^* & 0 & (\mathbf{i}\times\mathbf{j})\zeta_{\mathbf{i}} & (\mathbf{j}\times\mathbf{i})\zeta_{-\mathbf{k}} & 0 & 0^* \\
(\mathbf{i}\times\mathbf{j})\zeta_{-\mathbf{j}} & (\mathbf{j}\times\mathbf{i})\zeta_{-\mathbf{i}} & 0 & 0^* & 0^* & 0
\end{array}\right]
\end{array}, \tag{A.1}
$$

where star denotes matrix entries which are not zero in the original system, but contain dynamical variables that are not in the wave-triad subsystem. The structure matrix of the subsystem is clearly skew-symmetric, but the structure functions do not satisfy the Jacobi identity. This can be easily verified by substituting **i**, **j**, **–i** or **i**, **j**, **–j** for p, q, r in the Jacobi identity. Until this point, however, we did not make use of the reality condition, an important symmetry condition. Using of the reality condition the six-variable complex system can be replaced by an equivalent six-variable real system. The structure matrix for this real system is

$$
\begin{array}{c} \\ \mathbf{i}^r \\ \mathbf{j}^r \\ \mathbf{k}^r \\ \mathbf{i}^i \\ \mathbf{j}^i \\ \mathbf{k}^i \end{array}
\begin{array}{c}
\begin{array}{cccccc} \mathbf{i}^r & \mathbf{j}^r & \mathbf{k}^r & \mathbf{i}^i & \mathbf{j}^i & \mathbf{k}^i \end{array} \\
\begin{bmatrix}
0 & (\mathbf{i}\times\mathbf{j})\zeta_{\mathbf{k}^r} & (\mathbf{j}\times\mathbf{i})\zeta_{\mathbf{j}^r} & 0 & (\mathbf{i}\times\mathbf{j})\zeta_{\mathbf{k}^i} & (\mathbf{j}\times\mathbf{i})\zeta_{\mathbf{j}^i} \\
(\mathbf{j}\times\mathbf{i})\zeta_{\mathbf{k}^r} & 0 & (\mathbf{i}\times\mathbf{j})\zeta_{\mathbf{i}^r} & (\mathbf{j}\times\mathbf{i})\zeta_{\mathbf{k}^i} & 0 & (\mathbf{i}\times\mathbf{j})\zeta_{\mathbf{i}^i} \\
(\mathbf{i}\times\mathbf{j})\zeta_{\mathbf{j}^r} & (\mathbf{j}\times\mathbf{i})\zeta_{\mathbf{i}^r} & 0 & (\mathbf{j}\times\mathbf{i})\zeta_{\mathbf{j}^i} & (\mathbf{i}\times\mathbf{j})\zeta_{\mathbf{i}^i} & 0 \\
0 & (\mathbf{i}\times\mathbf{j})\zeta_{\mathbf{k}^i} & (\mathbf{i}\times\mathbf{j})\zeta_{\mathbf{j}^i} & 0 & (\mathbf{j}\times\mathbf{i})\zeta_{\mathbf{k}^r} & (\mathbf{j}\times\mathbf{i})\zeta_{\mathbf{j}^r} \\
(\mathbf{j}\times\mathbf{i})\zeta_{\mathbf{k}^i} & 0 & (\mathbf{j}\times\mathbf{i})\zeta_{\mathbf{i}^i} & (\mathbf{i}\times\mathbf{j})\zeta_{\mathbf{k}^r} & 0 & (\mathbf{i}\times\mathbf{j})\zeta_{\mathbf{i}^r} \\
(\mathbf{i}\times\mathbf{j})\zeta_{\mathbf{j}^i} & (\mathbf{j}\times\mathbf{i})\zeta_{\mathbf{i}^i} & 0 & (\mathbf{i}\times\mathbf{j})\zeta_{\mathbf{j}^r} & (\mathbf{j}\times\mathbf{i})\zeta_{\mathbf{i}^r} & 0
\end{bmatrix}
\end{array}, \tag{A.2}
$$

where the real variables $\zeta_{\mathbf{n}^i}$ and $\zeta_{\mathbf{n}^r}$ are defined as $\zeta_{\mathbf{n}} = \zeta_{\mathbf{n}^i} + i\zeta_{\mathbf{n}^r}$ (i is the imaginary unit).

Unless all imaginary components are zero the Jacobi identity cannot be satisfied. This follows from Eq. (5) of Part I upon substitution of e.g. $\mathbf{i}^r$, $\mathbf{j}^r$, $\mathbf{i}^i$ for p, q, r:

$$
\begin{aligned}
\sum_{x=i,r}\sum_{\mathbf{l}^x}\left\{D_{\mathbf{i}^r\mathbf{l}^x}\frac{\partial D_{\mathbf{j}^r\mathbf{i}^i}}{\partial\zeta_{\mathbf{l}^x}} + D_{\mathbf{i}^i\mathbf{l}^x}\frac{\partial D_{\mathbf{i}^r\mathbf{j}^r}}{\partial\zeta_{\mathbf{l}^x}} + D_{\mathbf{j}^r\mathbf{l}^x}\frac{\partial D_{\mathbf{i}^i\mathbf{i}^r}}{\partial\zeta_{\mathbf{l}^x}}\right\} \\
= \left[(\mathbf{j}\times\mathbf{i})^2\zeta_{\mathbf{j}^i} + (\mathbf{i}\times\mathbf{j})^2\zeta_{\mathbf{j}^i}\right] \\
= 2(\mathbf{j}\times\mathbf{i})^2\zeta_{\mathbf{j}^i} = 0, \quad \text{only if } \zeta_{\mathbf{j}^i} = 0.
\end{aligned} \tag{A.3}
$$

Similarly, replacing p, q and r by the index triads $\mathbf{j}^r$, $\mathbf{i}^r$, $\mathbf{j}^i$ and $\mathbf{i}^r$, $\mathbf{k}^r$, $\mathbf{i}^i$ would require the vanishing of $\zeta_{\mathbf{j}^i}$ and $\zeta_{\mathbf{k}^i}$, respectively.

On the other hand for purely real components the structure matrix reduces to

$$
\begin{array}{c} \\ \mathbf{i}^r \\ \mathbf{j}^r \\ \mathbf{k}^r \end{array}
\begin{array}{c}
\begin{array}{ccc} \mathbf{i}^r & \mathbf{j}^r & \mathbf{k}^r \end{array} \\
\begin{bmatrix}
0 & (\mathbf{i}\times\mathbf{j})\zeta_{\mathbf{k}^r} & (\mathbf{j}\times\mathbf{i})\zeta_{\mathbf{j}^r} \\
(\mathbf{j}\times\mathbf{i})\zeta_{\mathbf{k}^r} & 0 & (\mathbf{i}\times\mathbf{j})\zeta_{\mathbf{i}^r} \\
(\mathbf{i}\times\mathbf{j})\zeta_{\mathbf{j}^r} & (\mathbf{j}\times\mathbf{i})\zeta_{\mathbf{i}^r} & 0
\end{bmatrix}
\end{array}, \tag{A.4}
$$

and the structure functions can be easily shown to satisfy the Jacobi condition. Thus property (*i*) is proved. Note that an analogue statement for a system consisting of purely imaginary components is not valid because the structure functions describing interactions between the imaginary parts contain real variables.

Conservation of energy follows from the skew-symmetry of the structure matrix, while the conservation of enstrophy is the consequence of

$$\sum_{x=r,i}\sum_{\mathbf{k}^x} D_{\mathbf{l}\mathbf{k}^x}\zeta_{\mathbf{k}^x} = 0 \quad \text{for} \quad l \in \{\mathbf{i}^r,\mathbf{j}^r,\mathbf{k}^r,\mathbf{i}^i,\mathbf{j}^i,\mathbf{k}^i\}, \tag{A.5}$$

which is equivalent to Eq. (2) applied to the enstrophy $C^2 = \sum_{x=r,i}\sum_{\mathbf{k}^x} \zeta^2_{\mathbf{k}^x}$.

Feature *(i)* of the above lemma has the following important consequence:

Corollary: *An aliasing-free truncation inevitably destroys the Hamiltonian structure.*

Proof: An aliasing-free truncated system can be decomposed into a collection of wave triads. The skew-symmetry of the structure matrices of the wave-triad subsystems guarantees the skew-symmetry of the structure matrix of the complete truncated system. The truncated system, however, is not Hamiltonian, since there are wave triads, for which the "stared" coefficients of A.1 still contain wave vectors out of the lattice and must be replaced by zero. An example for such wave triad is $\mathbf{i} = (T-1, T)$, $\mathbf{j} = (1, -1)$ and $\mathbf{k} = (T, T-1)$. If $T \geq 2$, the spectral coefficients associated with the wave vectors $\mathbf{i}+\mathbf{k}$, $\mathbf{i}-\mathbf{j}$, $\mathbf{j}+\mathbf{k}$, $\mathbf{j}-\mathbf{i}$, $\mathbf{k}+\mathbf{i}$, $\mathbf{k}+\mathbf{j}$, $-\mathbf{i}+\mathbf{j}$, $-\mathbf{i}-\mathbf{k}$, $-\mathbf{j}+\mathbf{i}$, $-\mathbf{j}-\mathbf{k}$, $-\mathbf{k}-\mathbf{i}$ and $-\mathbf{k}-\mathbf{j}$ are definitely out of the truncation. At $T = 1$ the wave vectors $\mathbf{i}+\mathbf{k}$, $\mathbf{k}+\mathbf{i}$, $-\mathbf{i}-\mathbf{k}$, $-\mathbf{k}-\mathbf{i}$ are within the lattice, thus the structure matrix for this subsystem contains additional terms compared to A.1. The following entries of the structure matrix differs from that of a single wave-triad (A.2):

$$\begin{aligned}
&D_{\mathbf{i}^r\mathbf{k}^r} = (\mathbf{j}\times\mathbf{i})(\zeta_{\mathbf{j}^r} - \zeta_{(\mathbf{i}+\mathbf{k})^r}), \quad && D_{\mathbf{i}^r\mathbf{k}^i} = (\mathbf{j}\times\mathbf{i})(\zeta_{\mathbf{j}^i} - \zeta_{(\mathbf{i}+\mathbf{k})^i}),\\
&D_{\mathbf{k}^r\mathbf{i}^r} = (\mathbf{i}\times\mathbf{j})(\zeta_{\mathbf{j}^r} - \zeta_{(\mathbf{i}+\mathbf{k})^r}), \quad && D_{\mathbf{k}^r\mathbf{i}^i} = (\mathbf{j}\times\mathbf{i})(\zeta_{\mathbf{j}^i} + \zeta_{(\mathbf{i}+\mathbf{k})^i}),\\
&D_{\mathbf{i}^i\mathbf{k}^r} = (\mathbf{i}\times\mathbf{j})(\zeta_{\mathbf{j}^i} + \zeta_{(\mathbf{i}+\mathbf{k})^i}), \quad && D_{\mathbf{i}^i\mathbf{k}^i} = (\mathbf{j}\times\mathbf{i})(\zeta_{\mathbf{j}^r} + \zeta_{(\mathbf{i}+\mathbf{k})^r}),\\
&D_{\mathbf{k}^i\mathbf{i}^r} = (\mathbf{i}\times\mathbf{j})(\zeta_{\mathbf{j}^i} - \zeta_{(\mathbf{i}+\mathbf{k})^i}), \quad && D_{\mathbf{k}^i\mathbf{i}^i} = (\mathbf{i}\times\mathbf{j})(\zeta_{\mathbf{j}^r} + \zeta_{(\mathbf{i}+\mathbf{k})^r}).
\end{aligned} \tag{A.6}$$

Again it is possible to find index vectors for which the Jacobi identity fails. Let $p = \mathbf{i}^r$, $q = \mathbf{j}^r$ and $r = \mathbf{i}^i$ then

$$\begin{aligned}
&\sum_{x=i,r}\sum_{\mathbf{l}^x}\left\{D_{\mathbf{i}^r\mathbf{l}^x}\frac{\partial D_{\mathbf{j}^r\mathbf{i}^i}}{\partial\zeta_{\mathbf{l}^x}} + D_{\mathbf{i}^i\mathbf{l}^x}\frac{\partial D_{\mathbf{i}^r\mathbf{j}^r}}{\partial\zeta_{\mathbf{l}^x}} + D_{\mathbf{j}^r\mathbf{l}^x}\frac{\partial D_{\mathbf{i}^i\mathbf{i}^r}}{\partial\zeta_{\mathbf{l}^x}}\right\}\\
&= (\mathbf{j}\times\mathbf{i})\left[(\mathbf{j}\times\mathbf{i})\zeta_{\mathbf{j}^i} + (\mathbf{i}\times\mathbf{j})\zeta_{(\mathbf{i}+\mathbf{k})^i}\right] + (\mathbf{i}\times\mathbf{j})\left[(\mathbf{i}\times\mathbf{j})\zeta_{\mathbf{j}^i} + (\mathbf{i}\times\mathbf{j})\zeta_{(\mathbf{i}+\mathbf{k})^i}\right]\\
&= 2(\mathbf{j}\times\mathbf{i})^2\zeta_{\mathbf{j}^i} \neq 0.
\end{aligned} \tag{A.7}$$

Appendix B

We show that

$$C^N = \sum_{\sum_{i=1}^{N} \mathbf{n}_i = \mathbf{0}} \zeta_{\mathbf{n}_1} \cdots \zeta_{\mathbf{n}_N}. \tag{B.1}$$

is not conserved in the aliasing-free truncation if $N > 2$.
If C^N were a Casimir invariant, Eq. (2) would imply that

$$\left[\mathbf{D} \frac{\partial C^N}{\partial \zeta} \right]_{\mathbf{k}} = 0 \tag{B.2}$$

should be valid for each $\mathbf{k} \in I$.

Using the definitions of the structure functions (Eq. 10) and Eq. (B.1) the left-hand side of Eq. (B.2) reads

$$\sum_{\mathbf{i} \in I} \mathbf{D}_{\mathbf{ki}} \frac{\partial C^N}{\partial \zeta_{\mathbf{i}}} = N \sum_{\substack{\mathbf{i} \in I \\ \mathbf{i}+\mathbf{k} \in I}} \sum_{\substack{N-1 \\ \sum_{j=1} \mathbf{m}_j = -\mathbf{i}}} (\mathbf{k} \times (\mathbf{i}+\mathbf{k})) \zeta_{\mathbf{i}+\mathbf{k}} \zeta_{\mathbf{m}_1} \cdots \zeta_{\mathbf{m}_{N-1}}. \tag{B.3}$$

This double sum contains N-fold products of $\zeta_{\mathbf{e}_i}$-s that obey $\sum_{i=1}^{N} \mathbf{e}_i = \mathbf{k}$ and $\mathbf{e}_i - \mathbf{k} \in I$. If the latter condition holds for all indices in the set $\{\mathbf{e}_1, \ldots, \mathbf{e}_N\}$ then the subsum of the N-fold products containing these $\zeta_{\mathbf{e}_i}$-s in all possible permutations is zero, as it was shown in the main body of the paper (see Eq. (14)). But in case of most index sets the second condition is not valid for all $\mathbf{e}_i$ in the index set, and the summation takes the form

$$\sum_{\{\mathbf{e}_i\} \in P_N^{\mathbf{k}}} \zeta_{\mathbf{e}_1} \cdots \zeta_{\mathbf{e}_N} R^{\mathbf{k}}(\mathbf{e}_1, \ldots, \mathbf{e}_N), \tag{B.4}$$

where $R^{\mathbf{k}}(\mathbf{e}_1, \ldots, \mathbf{e}_N) = \sum_{\substack{i=1 \\ \mathbf{e}_i - \mathbf{k} \in I}}^{N} \mathbf{k} \times \mathbf{e}_i (N-1)!$. We prove that this sum cannot be zero for all vorticity fields.

Suppose that Eq. (B.4) is zero for all possible spectral coefficients. Let L denote the number of $\{\mathbf{e}_i\}$ sets in $P_N^{\mathbf{k}}$ and let us specify L different vorticity fields. Let p_i be different prime integers greater than N for $i=1,...,(M^2-1)$. Introducing new indices $r: I \to \{1,...,(M^2-1)/2\}$ that satisfy $r(\mathbf{e}) = r(-\mathbf{e})$ for each $\mathbf{e} \in I$, let $\zeta_{\mathbf{e}_i}^{(l)} = \exp(il\nu_{r(\mathbf{e}_i)})$ and $\zeta_{-\mathbf{e}_i}^{(l)} = \exp(-il\nu_{r(\mathbf{e}_i)})$, where $\nu_{r(\mathbf{e}_i)} = 2\pi/p_{r(\mathbf{e}_i)}$ and $l \in \{0,1,...,L-1\}$. This choice guarantees that the N-fold products $\zeta_{\mathbf{e}_1}^{(1)} \cdots \zeta_{\mathbf{e}_N}^{(1)}$, are all distinct. Let $a_j = \zeta_{\mathbf{e}_{j_1}}^{(1)} \cdots \zeta_{\mathbf{e}_{j_N}}^{(1)}$. The condition that Eq. (B.4) is zero for the vorticity fields just defined yields a homogeneous system of linear equations for $R^{\mathbf{k}}(\mathbf{e}_1,...,\mathbf{e}_N)$-s with constant coefficients:

$$\begin{bmatrix} 1 & 1 & ... & 1 \\ a_1 & a_2 & ... & a_L \\ a_1^2 & a_2^2 & ... & a_L^2 \\ ... & ... & ... & ... \\ a_1^{L-1} & a_2^{L-1} & ... & a_L^{L-1} \end{bmatrix}. \tag{B.5}$$

Since the a_i-s are distinct the coefficients form a nonsingular Vandermonde determinant and the system of equation has only trivial solution, that is all $R^{\mathbf{k}}(\mathbf{e}_1,...,\mathbf{e}_N)$-s should be zero. On the other hand it is easy to construct examples of $\{\mathbf{e}_i\}$ for nonzero $R^{\mathbf{k}}(\mathbf{e}_1,...,\mathbf{e}_N)$. Let $\mathbf{k} = (k_1,k_2)$ and suppose that $k_2 \geq 0$. Take the index set $\mathbf{e}_1 = (0, k_2 - T - 1)$, $\mathbf{e}_2 = (a,T)$ and $\mathbf{e}_3 = (k_1 - a, 1)$ where $|a|, |k_1 - a| \leq T$ and $\mathbf{e}_i = 0$ for $i = 4,...,N$. Since the first index $\mathbf{e}_1 - \mathbf{k}$ is out of the truncation, $R^{\mathbf{k}}(\mathbf{e}_1,...,\mathbf{e}_N) = \mathbf{k} \times (\mathbf{e}_2 + \mathbf{e}_3) = (T + k_2 + 1)k_1$ which is zero only if $k_1 = 0$. In the latter case, however, take $\mathbf{e}_1 = (0, k_2 - T - 1)$, $\mathbf{e}_2 = (0,T)$ and $\mathbf{e}_3 = (-1,1)$ and $R^{\mathbf{k}}$ will not vanish if $\mathbf{k} \neq \mathbf{0}$. The counter-example given shows that Eq. (B.4) cannot be zero for all vorticity fields.

Appendix C

Invariants of the sine-bracket truncation

As it is stated in a number of papers (e.g. *Zeitlin*, 1991; *Dowker* and *Wolski*, 1992) the truncated system Eq. (17) can be written in the equivalent "bracket form" of

$$\dot{\Omega} = \frac{i}{2\epsilon}[\Omega, \psi], \tag{C.1}$$

where i is the imaginary unit, ϵ is as defined in the main text, $\Omega(t) = \sum_{\mathbf{n}} \zeta_{\mathbf{n}}(t)\mathbf{J}_{\mathbf{n}}$, $\psi(t) = \sum_{\mathbf{n}} \frac{\zeta_{\mathbf{n}}(t)}{|\mathbf{n}|^2}\mathbf{J}_{\mathbf{n}}$ and $[.,.]$ denotes matrix commutation $[\Omega, \psi] = \Omega\psi - \psi\Omega$. The $\mathbf{J}_{\mathbf{n}}$-s are special $M \times M$ matrices (they are generators of the vector space of $M \times M$ Hermitian matrices) with the properties

$$\begin{aligned} \mathbf{J}_{\mathbf{n}} &= \mathbf{J}_{\mathbf{n}}^{*}, \\ \mathbf{J}_{\mathbf{n}}\mathbf{J}_{\mathbf{m}} &= exp(i\epsilon\,(\mathbf{m} \times \mathbf{n}))J_{\mathbf{n}+\mathbf{m} \bmod M}, \\ tr\mathbf{J}_{\mathbf{n}} &= \begin{cases} M & \text{for } \mathbf{n} = \mathbf{0} \\ 0 & \text{for } \mathbf{n} \neq \mathbf{0} \end{cases} \end{aligned} \tag{C.2}$$

Because of the multiplication rule Ω^N is also a linear combination of the $\mathbf{J}_{\mathbf{n}}$-s

$$\Omega^N = \sum_{\mathbf{i}} x_{\mathbf{i}}\mathbf{J}_{\mathbf{i}}. \tag{C.3}$$

Let $y_{\mathbf{j}} = \frac{\zeta_{\mathbf{j}}}{|\mathbf{j}|^2}$. From Eq. (C.1) and the properties of the $\mathbf{J}_{\mathbf{n}}$-s follows

$$\begin{aligned} \frac{\partial}{\partial t} tr\Omega^N &= tr\left([\Omega^N, \psi]\right) = tr\sum_{\mathbf{i}}\sum_{\mathbf{j}} x_{\mathbf{i}}y_{\mathbf{j}}[\mathbf{J}_{\mathbf{i}}, \mathbf{J}_{\mathbf{j}}] \\ &= -2i\sum_{\mathbf{i}}\sum_{\mathbf{j}} x_{\mathbf{i}}y_{\mathbf{j}} \sin\left(\epsilon\,(\mathbf{i} \times \mathbf{j})\right) tr\mathbf{J}_{\mathbf{i}+\mathbf{j} \bmod M} \\ &= -2i\,M\sum_{\mathbf{i}} x_{\mathbf{i}}y_{-\mathbf{i}} \sin\left(\epsilon\,(\mathbf{i} \times -\mathbf{i})\right) = 0. \end{aligned} \tag{C.4}$$

That is, the quantities $C_s^N = \frac{1}{M} tr\Omega^N$ are all conserved, though only $M-1$ of them are functionally independent (see e.g. *Zeitlin*, 1991). Due to the features of $\mathbf{J_n}$ matrices these invariants can be written in the following form

$$\begin{aligned} C_s^N &= \frac{1}{M} tr\left(\sum_{\mathbf{i}} \zeta_{\mathbf{i}} \mathbf{J}_{\mathbf{i}}\right)^N \\ &= \frac{1}{M} \sum_{\mathbf{i}_1,\ldots,\mathbf{i}_N} \zeta_{\mathbf{i}_1} \cdots \zeta_{\mathbf{i}_N} tr\left(\mathbf{J}_{\mathbf{i}_1} \cdots \mathbf{J}_{\mathbf{i}_N}\right) \\ &= \sum_{\sum_{j=1}^{N} \mathbf{i}_j = \mathbf{0} \, mod M} \zeta_{\mathbf{i}_1} \cdots \zeta_{\mathbf{i}_N} \exp\left(\epsilon 2A(\mathbf{i}_1,\ldots,\mathbf{i}_N)\right) \\ &= \sum_{\sum_{j=1}^{N} \mathbf{i}_j = \mathbf{0} \, mod M} \zeta_{\mathbf{i}_1} \cdots \zeta_{\mathbf{i}_N} \cos\left(\epsilon 2A(\mathbf{i}_1,\ldots,\mathbf{i}_N)\right). \end{aligned} \tag{C.5}$$

In the last equality the following symmetry of the area function was considered

$$A(\mathbf{i}_1,\ldots,\mathbf{i}_N) = -A(\mathbf{i}_N,\ldots,\mathbf{i}_1). \tag{C.6}$$

IDŐJÁRÁS

Quarterly Journal of the Hungarian Meteorological Service
Vol. 102, No. 2, April–June 1998, pp. 109–127

Land-surface hydrology parameterization in PROGSURF: Formulation and test with Cabauw data*

Ferenc Ács[1] and **Michael Hantel**[2]

[1]*Department of Meteorology, Eötvös Loránd University, H-1083 Budapest, Ludovika tér 2, Hungary; E-mail: acs@nimbus.elte.hu*

[2]*University of Vienna, Hohe Warte 38, A-1190 Vienna, Austria*

(Manucript received 5 May 1997; in final form 20 October 1997)

Abstract—The land-surface model PROGSURF (*Prognosis of Surface Fluxes*) is introduced and applied for analysing the water budget components at the station Cabauw in the Netherlands. PROGSURF gives the main emphasis to water budget modeling. All relevant water transport processes are treated: rainfall interception, canopy drainage, infiltration, surface runoff, soil water diffusion, root water uptake, evapotranspiration, conductance of water through roots and stems and subsurface runoff. Particular attention is paid to the parameterization of transpiration. The canopy surface resistance concept is applied by using Jarvis' empirical formula. The effect of available soil moisture is parameterized via leaf water potential. The soil moisture change is simulated by a 3-layer diffusion type model.

By running PROGSURF using the Cabauw data set we obtain the following main results: evapotranspiration and runoff is –435 and 338 mm/year, respectively; annual mean of root zone soil moisture content is 0.345 m^3/m^3. Seasonal changes of water balance components are also suitably reproduced. Evapotranspiration (and thus indirectly soil moisture content and runoff) are very sensitive to the parameterization of available soil moisture; this applies both to the annual value and the seasonal change of the sensitive quantities.

Furthermore, we compare our results with those of the PILPS (Project for Intercomparison of Land-Surface Parameterization Schemes) Phase 2(a) experiment. The comparison reveals that the differences in the specification of the relevant PROGSURF parameters can be as important as the differences in the structure of the PILPS models. The results of this study may thus be useful for optimizing the transpiration schemes used in land surface models.

Key-words: surface water budget, transpiration, available soil moisture, complexity versus simplicity.

---

* The paper was presented at the 22nd General Assembly of EGS, Vienna, 21–24 April, 1997.

1. Introduction

Many aspects of land-surface hydrology parameterization are still not well understood. For example, the heterogeneity effect in up- and downscaling, the mechanism of transpiration, and the parameterization of the interaction between transpiration and other surface water budget components need to be improved. On the other hand, there is a permanent background for all modeling efforts: the aspect of *complexity versus simplicity*.

In the present study some of these aspects are considered. The surface water budget components are analysed by the aid of the land-surface model PROGSURF (**Prog**nosis of **Sur**face **F**luxes), developed jointly at University of Vienna and Eötvös Loránd University, Budapest. Most ingredients of PROGSURF are standard. The model gives emphasis to the water budget comprising a total of 4 layers (vegetation layer plus three soil layers). Transpiration is parameterized using the canopy surface resistance concept in form of *Jarvis'* (1976) multiplicative formula. This implies specification of two governing relative conductances: one describing the *atmospheric demand* (relative stomatal conductance F_{ad}); and one describing the *available soil moisture* (relative stomatal conductance F_{ma}). The effect of atmospheric forcing (radiation, air humidity and temperature) upon stomatal functioning is condensed into F_{ad}. The available soil moisture (hereafter soil moisture availability) for evapotranspiration is represented by F_{ma}. Two possible formulations of F_{ma} are investigated; both represent the relation among transpiration, soil moisture content and runoff in a different manner. F_{ma} can be parameterized either via soil moisture content (*Noilhan* and *Planton*, 1989) or via leaf water potential (*Choudhury*, 1983; *Sellers* and *Dorman*, 1987; *Lynn* and *Carlson*, 1990; *Ács*, 1994). When parameterized with soil moisture content, there is no atmospheric demand effect represented in F_{ma}. When parameterized via leaf water potential, the effect of the atmosphere is also implicitly contained in F_{ma} (*De Ridder* and *Schayes*, 1997), in addition to being represented explicitly by F_{ad}.

This study has a threefold aim. First, we document PROGSURF's land-surface hydrology parameterization, including the parameterizations just mentioned. Second, for the Cabauw data we show that PROGSURF reproduces the annual mean as well as the annual course of the water budget components. Third, we demonstrate that transpiration (and thus soil moisture content and runoff too) is largely determined by the parameterization of F_{ma}. The numerical experiments are performed in off-line mode using Cabauw data set with different modes of PROGSURF.

The paper is organized as follows: the land-surface hydrology parameterization is described in the next section, the experimental site and the measurements are discussed in Section 3, the validation results are presented in Section 4 and the sensitivity experiments are discussed in Section 5. The conclusions are given in Section 6.

2. *The model*

The land-surface model PROGSURF is mostly based on previous work of Ács (*Ács et al.*, 1991; *Ács*, 1994; *Ács* and *Hantel*, 1997, 1998). Variables and geometry of the model are schematically presented on *Fig. 1*. The core of the scheme is a 2-layer temperature prediction of the vegetation-ground system based on the force-restore method (*Noilhan* and *Planton*, 1989), plus a 3-layer diffusion type soil moisture prediction. Due to the overlap of the vegetation-ground system and the soil system the total number of layers is 4. The vegetation-ground system contains a vegetation layer and a soil surface layer. The index v refers to the vegetation; we shall use the words *vegetation* and *canopy* synonymously. Evapotranspiration is parameterized using surface resistance concepts. The canopy surface resistance is evaluated using Jarvis' proposal for estimating soil moisture availability parameter via leaf water potential. The aerodynamic resistance is separately calculated above bare and vegetated soil surfaces using Monin-Obukhov's similarity theory taking into account the atmospheric stability.

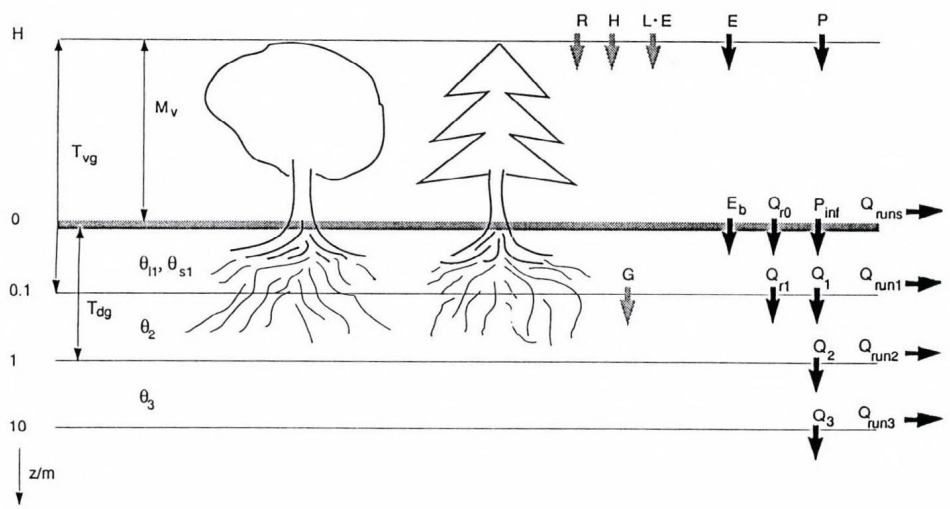

Fig. 1. Schematic diagram of prognostic variables, energy and water fluxes and layers represented by PROGSURF. (T_{vg} – temperature of vegetation-ground layer; T_{dg} – temperature of deep-ground layer; M_v – intercepted water stored in vegetation layer; θ_{l1}, θ_{s1} – liquid and solid water content in the 1st soil layer, respectively; θ_2, θ_3 – soil moisture content in the 2nd and 3rd layer; R – net radiation; H – sensible heat flux; $L \cdot E$ – latent heat flux; G – soil heat flux; E – moisture flux; E_b – bare soil evaporation; P – precipitation; Q_{r0}, Q_{r1} – root water flux across the surface and the bottom of the 1st layer; P_{inf}, Q_1, Q_2, Q_3 – soil water flux across the surface (infiltration) and the bottom of the 1st, 2nd and 3rd layer; Q_{runs}, Q_{run1}, Q_{run2}, Q_{run3} – runoff from the surface and horizontal discharge from the 1st, 2nd and 3rd soil layer. Energy fluxes are shaded, water fluxes are black and all fluxes are positive in positive z-direction, represented by downward arrows.)

PROGSURF is able to treat the case of frozen soil while the representation of snow is presently missing. Sub-gridscale variations of surface characteristics are not considered. We follow the convention to count all vertical fluxes to be positive if directed downwards. This implies, e.g., that the sign of evaporation and transpiration is practically always negative. In the following more attention is paid to the land-surface hydrology parameterization.

2.1 Soil moisture prediction

Diffusion-type moisture prediction is applied in the soil layers. The prognostic equations for the three layers (Fig. 1) are:

$$\rho_w \cdot D_1 \cdot \frac{\partial \theta_{l1}}{\partial t} = P_{\text{inf}} - Q_1 - Q_{r0} - Q_{r1} + E_b - Q_{run1} - S_p, \tag{1}$$

$$\rho_w \cdot D_1 \cdot \frac{\partial \theta_{s1}}{\partial t} = S_p, \tag{2}$$

$$\rho_w \cdot D_2 \cdot \frac{\partial \theta_2}{\partial t} = Q_1 - Q_2 + Q_{r1} - Q_{run2}, \tag{3}$$

$$\rho_w \cdot D_3 \cdot \frac{\partial \theta_3}{\partial t} = Q_2 - Q_3 - Q_{runs}, \tag{4}$$

where ρ_w is water density; D_i is the thickness of the ith soil layer; θ_{l1}, θ_{s1} is the liquid and solid moisture content in the 1st soil layer, respectively; θ_2, θ_3 is the soil moisture content in the 2nd and 3rd soil layer, respectively; P_{inf} is the water infiltrated into the soil (kg m^{-2} s^{-1}); E_b is the evaporation from bare soil surface (kg m^{-2} s^{-1}); Q_{r0} and Q_{r1} is the root water flux across surface and across the bottom of the 1st soil layer (kg m^{-2} s^{-1}); Q_1 and Q_2 is the water diffusion between the adjacent layers (kg m^{-2} s^{-1}); Q_3 is the gravitational drainage (kg m^{-2} s^{-1}) and Q_{runi} represents the lateral drainage in the ith layer (kg m^{-2} s^{-1}). Soil water diffusion terms are positive downwards and negative upwards. The gravitational and lateral drainage terms are positive representing the outflow from the system. S_p is the source/sink term (kg m^{-2} s^{-1}) representing soil water freezing or melting. It can be expressed as $S_p = -(R + H + L \cdot E - G)/L_f$, where R is the net radiation, H is the sensible heat flux, $L \cdot E$ is the latent heat flux, G is the soil heat flux and L_f is the latent heat of fusion. $S_p > 0$ when freezing and $S_p < 0$ when melting.

2.2 Water fluxes

The governing water transport processes in the soil-vegetation-atmosphere system are the precipitation, the rainfall interception, the canopy drainage, the distribution of the effective precipitation into the infiltration and surface runoff, the vertical water movement in the soil, the root water fluxes, the evapotranspiration, the conductance of water through roots and stems and the subsurface runoff. In the following the parameterizations of these processes are briefly presented.

2.2.1 Effective precipitation, infiltration and surface runoff

The effective precipitation rate on the soil surface (P_0) is defined by

$$P_0 = P - P_v + D_v, \tag{5}$$

where P is the rainfall intensity (kg m^{-2} s^{-1}), P_v is its interception by vegetation and D_v is the water drainage from the canopy. Both latter terms are parameterized after *Sellers et al.* (1986). P_0 either infiltrates into the soil (P_{inf}) or runs off on the surface (Q_{runs}) depending upon surface characteristics. This partition mechanism is parameterized as

$$P_{\text{inf}} = \begin{cases} \min(P_0, K_{S1}) & \text{if } W_1 < 1 \\ 0 & \text{if } W_1 = 1, \end{cases} \tag{6}$$

$$Q_{runs} = \begin{cases} P_0 & \text{if } W_1 = 1 \\ P_0 - K_{S1} & \text{if } W_1 < 1 \text{ and } P_0 > K_{S1} \\ 0 & \text{if } W_1 < 1 \text{ and } P_0 \leq K_{S1}, \end{cases} \tag{7}$$

where $W_1 = \theta_1/\theta_{S1}$; θ_{S1} is the saturated soil moisture content (m^3/m^3) and K_{S1} is the saturated hydraulic conductivity (kg m^{-2} s^{-1}) in the 1st soil layer. The parameterization does not take into account the orographical effects.

2.2.2 Evaporation and soil water transfer

Evaporation from bare soil is estimated by the aerodynamic formula evaluating soil surface resistance after *Sun* (1982). The water flow between the adjacent soil layers is estimated by

$$Q_i = K_{eff,i} \cdot \left[2 \cdot \frac{\Psi_i - \Psi_{i+1}}{D_i + D_{i+1}} + 1 \right], \tag{8}$$

$$K_{eff,i} = \frac{D_i \cdot K_i + D_{i+1} \cdot K_{i+1}}{D_i + D_{i+1}}, \tag{9}$$

where $K_{eff,i}$ is an effective hydraulic conductivity between the ith and $(i+1)$th ($i = 1, 2$) soil layers (kg m^{-2} s^{-1}), K_i is the hydraulic conductivity of the ith soil layer (kg m^{-2} s^{-1}) and Ψ_i is the soil water potential of the ith soil layer (m). Both latter terms are parameterized after *Clapp* and *Hornberger* (1978).

2.2.3 Water transfer in roots, stems and leaves

The root water flux (Q_{r0}) across the surface (kg m^{-2} s^{-1}) is assumed to flow in the stems of plants. The continuity of water flow in soil–vegetation–atmosphere system requires to equate Q_{r0} with the transpiration (E_{vd}):

$$E_{vd} = \frac{\rho c_p}{L\gamma} \cdot \frac{e_S(T_{vg}) - e_r}{r_v + r_{av}}, \tag{10}$$

$$Q_{r0} = E_{vd}, \tag{11}$$

where ρ is the air density (kg/m^3), c_p is the specific heat of air at constant pressure (J kg^{-1} K^{-1}), γ is the psychrometric constant (hPa/K), $e_S(T_{vg})$ is the saturation vapor pressure at T_{vg} (hPa), e_r is the vapor pressure at reference level (hPa), r_v is the canopy resistance (s/m) and r_{av} is the aerodynamic resistance above vegetation (s/m).

The root water flux (Q_{r1}) across the bottom of the 1st layer is estimated as a prespecified percentage of the flux across the ground surface (*Chen et al.*, 1997):

$$Q_{r1} = 0.3 \cdot Q_{r0}. \tag{12}$$

Q_{r0} is parameterized using leaf water potential (Ψ_v) according to *van der Hornert* (1948):

$$Q_{r0} = \rho_w \cdot \frac{\Psi_v - \Psi_R + z_T}{r_R + r_P}, \tag{13}$$

where Ψ_R is the soil moisture potential in the root zone (m), z_T is the canopy source-sink height (m), r_R is the soil resistance in the root zone (s) and r_P is the plant resistance imposed by the plant vascular system (s). r_P depends on vegetation type; in our tests we used PILPS specified value of 2.5×10^8 s.

2.2.4. *Subsurface runoff*

Subsurface runoff is the sum of lateral and gravitational drainage. Lateral drainage is estimated for each soil layer ($i = 1, 2, 3$) using the expressions

$$Q_{runi} = \begin{cases} Q_{rfi} & \text{if } WFC_i \leq 0 \\ Q_{rfi} + WF_i & \text{if } WFC_i > 0, \end{cases} \tag{14}$$

where

$$Q_{rfi} = Q_i - \min(Q_i, K_{Si}), \tag{15}$$

$$WF_1 = P_{\text{inf}} - Q_1 + E_b + Q_{r0} - Q_{r1} - Q_{rf1}, \tag{16}$$

$$WF_2 = Q_1 - Q_2 + Q_{r1} - Q_{rf2}, \tag{17}$$

$$WF_3 = Q_2 - Q_3 - Q_{rf3}, \tag{18}$$

$$WFC_i = \frac{\rho_w D_i}{\Delta t} \cdot (\theta_i - \theta_{fi}) + WF_i, \tag{19}$$

where Δt is the time step, θ_i is the actual soil moisture content and θ_{fi} is the soil moisture content at field capacity in the ith soil layer; WF_i represents the net water flux in the ith soil layer and K_{Si} is the saturated hydraulic conductivity in the ith soil layer.

The gravitational drainage rate from the bottom (Q_3) is calculated by

$$Q_3 = \begin{cases} K_{S3} \cdot W_3^{2B_3+3} & \text{if } \theta_3 \geq \theta_{f3} \\ 0 & \text{if } \theta < \theta_{f3} \end{cases}, \tag{20}$$

where W_3 is defined equivalently to W_1 (see Eq. (7)).

2.3 Resistances

To estimate evapotranspiration, it is necessary to determine aerodynamic and surface resistances. The aerodynamic resistance is evaluated using Monin-Obukhov's similarity theory taking into account the atmospheric stability. It is split into laminar and turbulent terms distinguishing transports between momentum and heat/moisture. It is separately calculated above bare and vegetated soil surfaces. Here the attention is paid only to the canopy surface resistance formulation.

2.3.1 Canopy resistance

Canopy resistance is parameterized following *Jarvis*' method (1976):

$$r_v = \frac{r_{st\,\min} \cdot F_{ad}}{LAI \cdot GLF \cdot F_{ma}}, \tag{21}$$

where r_{stmin} is the minimum stomatal resistance at optimal environmental conditions, *LAI* is the leaf area index (m^2/m^2) and *GLF* is the green leaf fraction (it expresses the fraction of green leaves ranging from 0 to 1; for parameter values see Table A2 in *Chen et al.*, 1997). F_{ad} and F_{ma} expresses the atmospheric demand and the soil moisture availability effect upon stomatal activity, respectively.

F_{ad} is split into three effects in a multiplicative manner:

$$F_{ad} = \frac{F_{vr}}{F_{ah} \cdot F_{at}}, \tag{22}$$

where F_{vr}, F_{ah} and F_{at} expresses the influence of absorbed visible radiation, air humidity and temperature, respectively. F_{vr} is parameterized after *Gates* (1981) while F_{ah} and F_{at} after *Jarvis* (1976) and *Dickinson* (1984).

F_{ma} is parameterized via leaf water potential as:

$$F_{ma} = \frac{\Psi_v - \Psi_{cr}}{\Psi_{SR} - \Psi_{cr}}, \tag{23}$$

where Ψ_v and Ψ_{cr} is the actual and the critical leaf water potential (m), respectively. At $\Psi_v = \Psi_{cr}$ the stomata are completely closed. Ψ_{cr} depends on vegetation type; for grass it is –230 m. Ψ_{SR} is the saturated soil water potential in the root zone (m); it is estimated as the weighted mean of Ψ_{S1} and Ψ_{S2} (for their values see Table A1 in *Chen et al.*, 1997) as follows:

$$\Psi_{SR} = \frac{D_1 \Psi_{S1} + D_2 \Psi_{S2}}{D_1 + D_2}. \tag{24}$$

To apply Eq. (23), it is necessary to determine Ψ_v. Combining Eqs. (10), (11), (13), (21) and Eq. (23) and after some rearranging, it is possible to get a quadratic equation for Ψ_v:

$$a \cdot \Psi_v^2 + b \cdot \Psi_v + c = 0, \tag{25}$$

where

$$a = r_{av}, \tag{26}$$

$$b = AD \cdot (r_R + r_P) - (\Psi_R - z_T) \cdot r_{av} + A \cdot (\Psi_{SR} - \Psi_{cr}) - \Psi_{cr} \cdot r_{av}, \tag{27}$$

$$c' = -AD \cdot (r_R + r_P) \cdot \Psi_{cr} + (\Psi_R - z_T) \cdot \Psi_{cr} \cdot r_{av}, \tag{28}$$

$$c = c' - A \cdot (\Psi_R - z_T) \cdot (\Psi_{SR} - \Psi_{cr}), \tag{29}$$

and

$$AD = \frac{\rho c_p}{\gamma L \rho_w} \cdot veg \cdot (1 - wif) \cdot [e_S(T_{vg}) - e_r], \tag{30}$$

$$A = \frac{r_{stmin} \cdot F_{ad}}{LAI \cdot GLF}. \tag{31}$$

The soil resistance in the root zone (r_R) is expressed as

$$r_R = \frac{\alpha_R \cdot \rho_w}{K_R \cdot D_R}, \tag{32}$$

where K_R is the hydraulic conductivity of soil in the root zone (kg m^{-2} s^{-1}), D_R is the root zone depth taken as 1 m. α_R is a vegetation specific parameter for the root zone (m^2), given by

$$\alpha_R = \frac{V_R - 3 - 2 \cdot \log\left[\frac{V_R}{1 - V_R}\right]}{8 \cdot \pi \cdot R_{\mathrm{det}}}, \tag{33}$$

where V_R is the volume of root per unit volume of soil in the root zone (m^3/m^3). Term V_R is estimated from the total root density in the root zone (R_{det}) and from the average root cross section (rcs). R_{det} is calculated after *Gerwitz* and *Page* (1974) when the root density in the soil surface layer (R_{des}) is known. For grass $R_{des} = 5500$ m/m^3 and $rcs = 3.84 \times 10^{-7}$ m^2. K_R and ψ_R are calculated as the weighted mean of their components analogously to Eq. (24).

The ψ_v value is obtained by solving Eq. (25),

$$\Psi_v = \frac{-b + [b^2 - 4 \cdot a \cdot c]^{1/2}}{2a}. \tag{34}$$

The other solution gives unrealistic results.

3. *The Cabauw data set*

There are three reasons for choosing data measured at Cabauw, the Netherlands in 1987:

(a) at Cabauw experimental station the measurements assured high quality values for the atmospheric forcing data, soil-vegetation parameters and the latent and sensible heat fluxes,

(b) the data series is long enough; it includes one full year providing a basis for testing model performance in terms of seasonal variations and

(c) the data set is chosen for the PILPS Phase 2(a) experiment which enables PROGSURF's comparison with other land-surface schemes.

Cabauw site is located in the Netherlands (51°58'N; 4°56'E); plant cover consists mainly of short grass with narrow ditches. The climate in the area is characterized as temperate maritime type with prevailing westerly winds. The soil consists of two layers: a 1-m-deep layer of silty clay on the top of a 10-m-deep layer of peat saturated with water. The most important soil hydraulic characteristics are presented in *Table 1*.

The Cabauw data, provided by the Royal Netherlands Meteorological Institute, are obtained in the scope of a semi-operational measurement program with a high level of quality control. The atmospheric forcing data (downward shortwave and longwave radiation, precipitation, surface atmospheric pressure,

near surface air humidity, temperature and wind speed) refer to the height of 20 m (reference height). For evaluation of scheme outputs, energy-flux data including sensible and latent heat fluxes, net radiation, upward longwave radiation and soil heat flux are available. The sensible and latent heat fluxes were not measured directly. The former was derived from temperature and wind profile data using modified flux-profile relationship while the latter is estimated as a residual of the surface energy balance (*Beljaars*, 1982). When any of the measurements for the energy-flux variables were not available, data were derived from a parameterization scheme which has been calibrated locally and tested extensively against observed data (*Holtslag* and *Van Ulden*, 1983). The Cabauw data used in the PILPS Phase 2(a) experiment refer and cover the entire year of 1987. Both the forcing data and the energy fluxes are available on a 30-min interval. The details are described in *Beljaars* and *Bosveld* (1997).

Table 1. Soil hydraulic characteristics at Cabauw site

Soil porosity	0.468
Soil moisture content at field capacity	0.370
Soil moisture content at wilting point	0.214
Saturated hydraulic conductivity (m/s)	3.4341×10^{-6}
Saturated soil water potential (m)	-0.045
'B' of *Clapp* and *Hornberger* (1978)	10.39

In the numerical experiments the PROGSURF is always initialized, as all schemes in PILPS 2(a) experiment, by saturating all liquid water stores and setting all temperatures to 279 K. The land-surface parameters are specified as designed in PILPS 2(a) comparison experiments (see Appendix in *Chen et al.* 1997).

4. Results of validation

The land-surface hydrology parameterization in PROGSURF is validated comparing (a) annual values of simulated and observed evapotranspiration and runoff and (b) annual course of simulated and observed evapotranspiration.

The annual partition of the amount of precipitation into evapotranspiration and runoff is presented on *Fig. 2*. In this case evapotranspiration *is practically*

equal to transpiration because the vegetation coverage is full. The results refer to the equilibrium year. Equilibrium was defined as being the first occasion that the January mean values of the surface temperature, latent and sensible heat fluxes and root-zone soil moisture did not change by more than 0.01 K, 0.1 W/m^2 and 0.1 mm, respectively, from year N to year N+1; the equilibrium time (spinup time) was then N years. PROGSURF's spinup time is 2 years.

The evapotranspiration and the runoff estimated by PROGSURF are -435 and 338 mm/year, respectively. The evapotranspiration and the runoff obtained by measurements and output analysis of the ECMWF (*European Centre for Medium-Range Weather Forecasts*) land-surface model (for details see *Viterbo* and *Beljaars*, 1995 and *Beljaars* and *Bosveld*, 1997) are about -525 and 250 mm/year, respectively.

The annual course of evapotranspiration simulated by PROGSURF (on the figure noted as Psi-PROGSURF) is presented on *Fig. 3*. The seasonal change of evapotranspiration is strong. In winter the values are small (around and under -10 mm/month); in summer they change between -70 and -100 mm/month. The absolute value of the maximum is 99 mm/month and appears in July. The root-mean-square error for simulated and observed values is 9.5 mm/month; it means that the agreement is suitable.

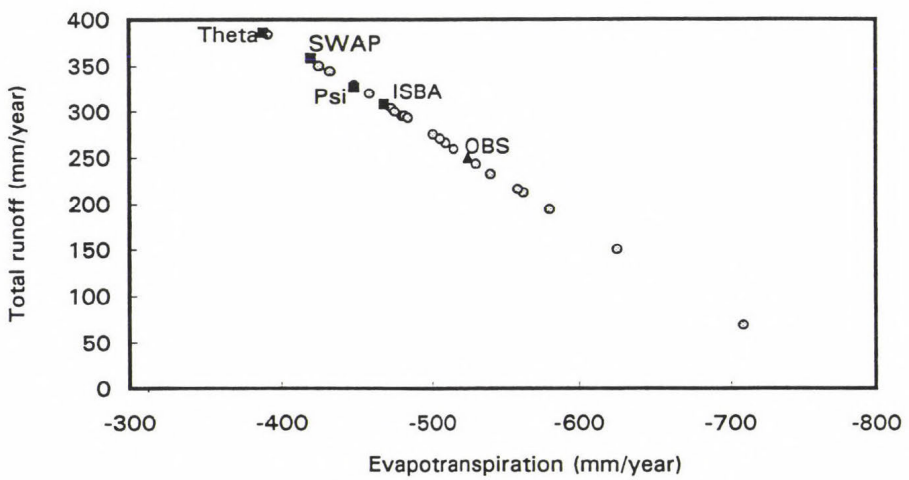

Fig. 2. Distribution of annual runoff and evapotranspiration at Cabauw experimental station in 1987. The estimations are obtained by the different versions of PROGSURF and by the models participating in PILPS Phase 2(a) experiment (for details see Fig. 10 in *Chen et al.*, 1997). *Psi* is a PROGSURF run with soil moisture availability parameter F_{ma} represented via leaf water potential; *Theta* is a PROGSURF run with F_{ma} represented via soil moisture contents; *ISBA* is a run with ISBA model; *SWAP* means a run with SWAP model; and *OBS* are the observed values.

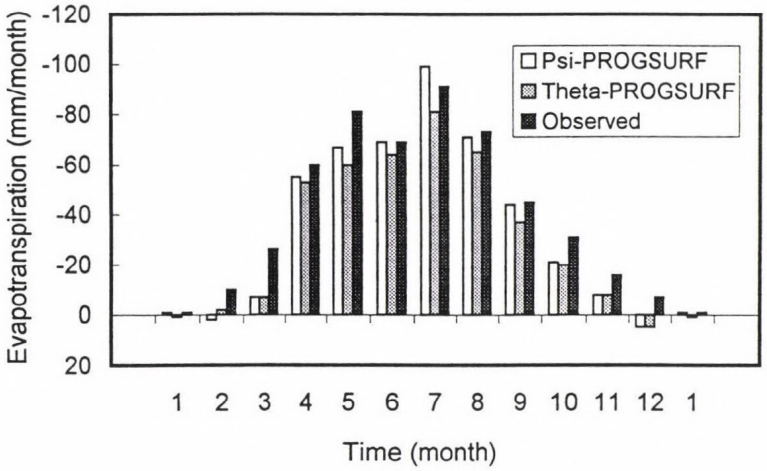

Fig. 3. Annual course of evapotranspiration simulated at Cabauw in 1987 by different versions of PROGSURF.

5. Sensitivity tests

In this chapter the sensitivity of the model performance to soil moisture availability (F_{ma}) formulation is tested. In PROGSURF, F_{ma} is estimated via leaf water potential. Both the soil moisture and the atmospheric demand effects (radiation, air temperature, humidity and aerodynamic resistances) are represented in this relatively complex formulation of F_{ma}.

Nevertheless, F_{ma} can also be parameterized in a very simple way via soil moisture contents

$$F_{ma} = \begin{cases} 1 & \text{for} \quad \theta_f \leq \theta \\ \dfrac{\theta - \theta_w}{\theta_f - \theta_w} & \text{for} \quad \theta_w < \theta < \theta_f, \\ 0 & \text{for} \quad \theta \leq \theta_w, \end{cases} \tag{35}$$

where θ, θ_f and θ_w is the actual, the field capacity and the wilting point soil moisture content in the root zone (m^3/m^3), respectively. The atmospheric demand effect is not represented in this formulation of F_{ma}.

A comparative analysis of two different versions of PROGSURF has been made to study the annual and seasonal characteristics of water budget

components from the aspect of *complexity versus simplicity*. In the Psi-PROGSURF version F_{ma} parameterized by Eq. (23), while Eq. (35) represents the parameterization of F_{ma} in the Theta-PROGSURF version.

5.1 Annual characteristics

The spinup time of Psi and Theta is 2 and 3 years, respectively. The distribution of precipitation between evapotranspiration and total runoff is presented on Fig. 2. The output obtained by Psi is in much better agreement with the observation than that estimated by Theta. The runoff produced by Theta is about 384 mm/year. In spite of this, Psi-PROGSURF's runoff is 338 mm/year which is closer to the observed value of 250 mm/year. Similarly, evapotranspiration obtained by Psi (–435 mm/year) is much closer to the observation (–522 mm/year) than the one obtained by Theta (–389 mm/year).

5.2 Seasonal changes of the water balance components

The monthly water budget is:

$$P_j + E_j + Q_{runj} = \Delta\Theta_j, \tag{36}$$

where j is the month index. P, E and Q_{run} are the monthly sum of precipitation, evapotranspiration and total runoff, respectively. Total runoff is the sum of the surface runoff Q_{runs} , subsurface lateral flows Q_{run1}, Q_{run2}, Q_{run3} and gravitational drainage Q_3. $\Delta\Theta$ is the change in total soil water storage (defined as $[\theta_1+\theta_2+\theta_3] \times 10$ m) from the beginning to the end of the month.

The annual course of observed precipitation is presented on *Fig. 4*. The annual course of E and Q_{run} obtained by the PROGSURF modes are presented on *Figs. 3* and *5*. The differences in evapotranspiration calculated by the modes are most pronounced in summer with a maximum in July. Theta-PROGSURF tends to underestimate the absolut value of the evapotranspiration as compared to the observation. The root-mean-square errors for Psi- and Theta-PROGSURF are 9.5 and 11.5 mm/month, respectively. Total runoff is mostly originated from the gravitational drainage. Q_{runs}, Q_{run1}, Q_{run2} and Q_{run3} are negligible, since their values are about 10 mm/year (not presented here). The annual amplitudes of E and Q_{run} simulated by Psi are greater than the ones simulated by Theta. During most of the winter (months 1–4) Q_{run} is between 35 and 45 mm/month, about the same for both runs. In summer Theta seems to overestimate the runoff as compared to Psi. Therefore the standard deviation of Q_{run} obtained by Psi (3.1 mm/month) is somewhat greater than the one obtained by Theta (2.3 mm/month).

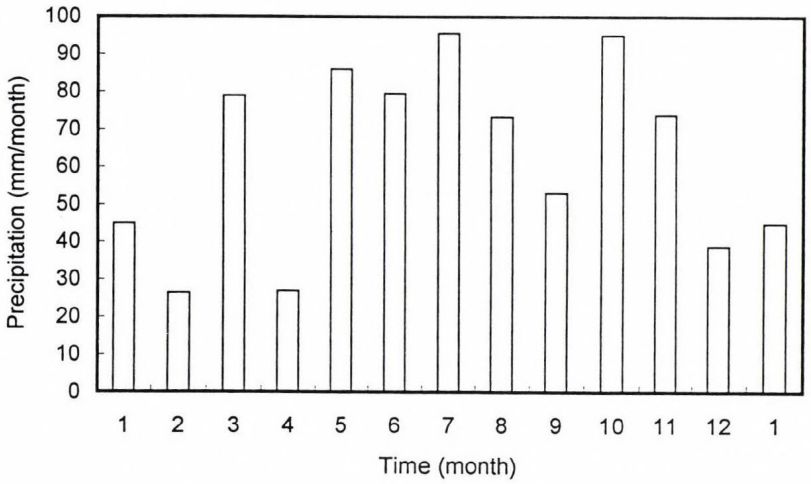

Fig. 4. Annual course of precipitation observed at Cabauw in 1987.

The annual course of soil water change in total soil depth (0–10 m) is presented in *Fig. 6*. Soil water change in total soil depth is significant in April and October. In April the soil water content decreases; in October the situation is reversed. The changes obtained by Theta are smaller than those of Psi. In summer the change is quite variable for both versions of PROGSURF. The standard deviation of $\Delta\Theta$ obtained by Psi and Theta is 3.9 and 4.0 mm/month, respectively.

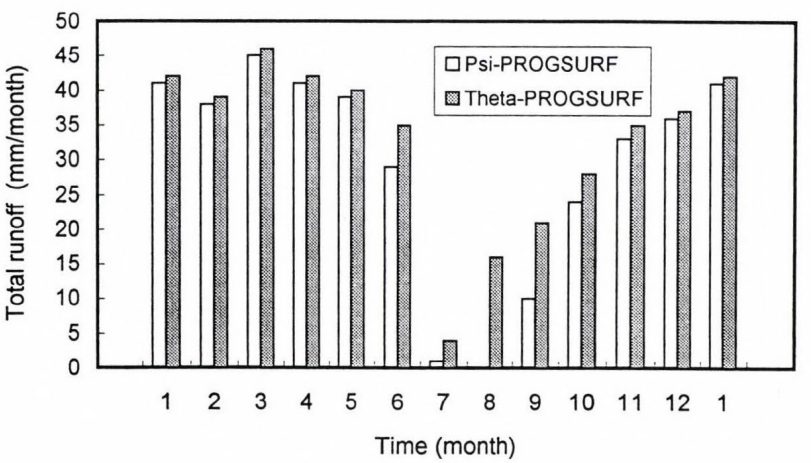

Fig. 5. Annual courses of total runoff.

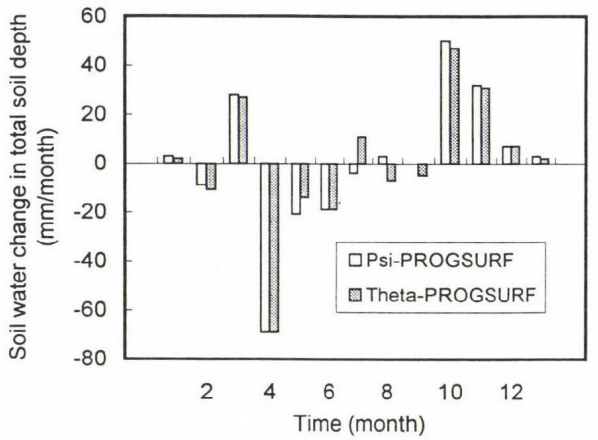

Fig. 6. Annual courses of soil water change in total soil depth of 10 m.

The annual course of soil water in the root-zone ($\theta_1 + \theta_2$, layers 0–1 m, see Fig. 1) is presented on *Fig. 7.* The annual course obtained by Psi-PROGSURF is between about 280 and 390 mm. The corresponding annual mean value is 345 mm. This is in accord with the other PILPS estimates (see Fig. 15 in *Chen et al.*, 1997). In summer, Theta overestimates soil water in the root-zone with respect to Psi. The standard deviation of $(\theta_1+\theta_2) \times 1$ m obtained by Psi and Theta is 12.2 and 11.6 mm, respectively.

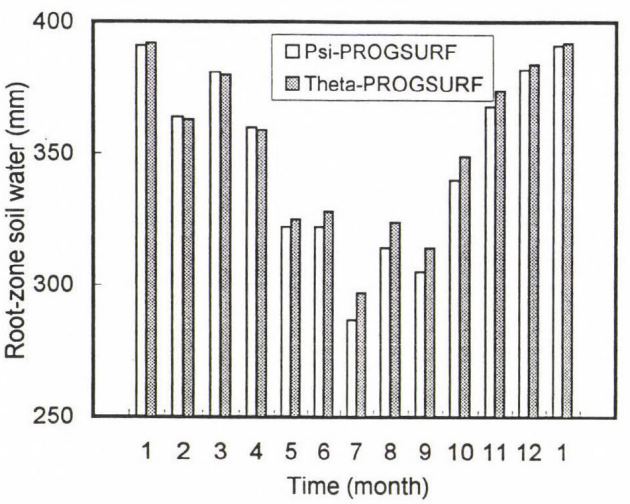

Fig. 7. Annual courses of root-zone soil water.

6. Conclusions

The land-surface hydrology parameterization in the model PROGSURF has been presented. PROGSURF contains 2 vegetation-soil layers and 3 soil layers; these systems overlap each other and represent a 4-layer model. Modeling of the transpiration is the core of the vegetation component. It is implemented using the canopy surface resistance concept with Jarvis' multiplicative formula. The moisture availability is parameterized via leaf water potential Ψ_v. Diffusion type soil moisture prediction is the core of the water transport module. Surface runoff is treated using both Horton and Dunne mechanisms (*Entekhabi* and *Eagleson*, 1989). Gravitational drainage is simply represented through soil water conductivity as parameterized by *Clapp–Hornberger*'s (1978) empirical formula.

PROGSURF has been run using the 1987 data from Cabauw, the Netherland, taking exactly the same specifications that have been applied in the PILPS campaign (*Chen et al.*, 1997). PROGSURF satisfactorily reproduces both the observed annual mean values and the seasonal changes of water fluxes and soil moisture content in the root zone. For example, the annual evapotranspiration and runoff is –435 and 338 mm, respectively. The corresponding observed values of E and Q_{run} are –522 and 250 mm.

The sensitivity of water budget components to different formulations of F_{ma} is also studied. The standard formulation of F_{ma} via leaf water potential (Psi-PROFSURF) is compared to F_{ma} represented by soil moisture contents (Theta-PROGSURF). When F_{ma} is parameterized with soil moisture contents, there is no atmospheric demand effect. On the other hand, when F_{ma} is parameterized via leaf water potential, the effect of the atmosphere is implicitly contained in F_{ma} (*De Ridder* and *Schayes*, 1997), in addition to being represented explicitly by F_{ad}. Our test results give pronounced differences for the water budget components. The deviation in evapotranspiration estimated by Psi- and Theta-PROGSURF is 58 mm/year. This value is as great as the deviations between some PILPS models of completely different structure (see Table 1 in *Chen et al.*, 1997). For example the difference in evapotranspiration between ISBA (Interaction Soil Biosphere Atmosphere) and SWAP (Soil Water-Atmosphere-Plant) is about 50 mm/year. These results suggest that the differences in the choice of the relevant PROGSURF parameters can be as important as the differences in the structure of a large class of land surface models like the ones studied in PILPS.

Further investigations are needed to understand the governing mechanism, which we have tried to represent in PROGSURF still better. Similar tests should also be performed for other climatic regions. It is hoped that further intercomparison campaigns presently in preparation may be useful for optimizing the transpiration subroutines seeking the balance between physics and complexity (*Henderson-Sellers et al.*, 1993).

Acknowledgements—The authors wish to thank the *Österreichische Akademie der Wissenschaften* within the National Austrian Committee for the IGBP and the *Hungarian Ministry for Culture and Education* under grant FKFP No. 0168/1997 for the financial support of this study. We thank *Dr. L. Haimberger* and *Dr. M. Dorninger* for their helpful discussions and help in data transfer processing. The technical help provided by *Mr. Z. Barcza* and by *Mrs. B. Berger* has been very constructive.

References

Ács, F., Mihailovic, D.T. and *Rajkovic, B.*, 1991: A coupled soil moisture and surface temperature prediction model. *J. Appl. Meteor. 30,* 812-822.

Ács, F., 1994: A coupled soil-vegetation scheme: description, parameters, validation, and sensitivity studies. *J. Appl. Meteor. 33*, 268-284.

Ács, F. and *Hantel, M.*, 1997: Transpiration – the relevant atmosphere-surface interaction process. *Book of Abstracts (Annales Geophysicae, Supplement II to Volume 15, Part II, Hydrology, Oceans, Atmosphere & Nonlinear Geophysics) of the 22nd General Assembly of the European Geophysical Society*, C 351.

Ács, F. and *Hantel, M.*, 1998: The land-surface flux model PROGSURF. Accepted in a special PILPS issue of *Global and Planetary Change*.

Beljaars, A.C.M., 1982: The derivation of the fluxes from profiles in perturbed areas. *Bound.-Layer Meteor. 24*, 35-55.

Beljaars, A.C.M. and *Bosveld, F.C.*, 1997: Cabauw data for the validation of land surface parameterization schemes. *J. Climate 10*, 1172-1194.

Chen, T.H., Henderson-Sellers, A., Milly, P.C.D., Pitman, A.J., Beljaars, A.C.M., Polcher, J., Abramopoulos, F., Boone, A., Chang, S., Chen, F., Dai, Y., Desborough, C.E., Dickinson, R.E., Dumenil, L., Ek, M., Garratt, J.R., Gedney, N., Gusev, Y.M., Kim, J., Koster, R., Kowalczyk, E.A., Laval, K., Lean, J., Lettenmaier, D., Liang, X., Mahfouf, J.-F., Mengelkamp, H.-T., Mitchell, K., Nasonova, O.N., Noilhan, J., Robock, A., Rosenzweig, C., Schaake, J., Schlosser, C.A., Schulz, J.-P., Shao, Y., Shmakin, A.B., Verseghy, D.L., Wetzel, P., Wood, E.F., Xue, Y., Yang, Z.-L. and *Zeng, Q.*, 1997: Cabauw experimental results from the project for intercomparison of land-surface parameterization schemes. *J. Climate 10,* 1194-1216.

Choudhury, B., 1983: Simulating the effects of weather variables and soil water potential on a corn canopy temperature. *Agric. Meteorol. 29*, 169-182.

Clapp, R.B. and *Hornberger, G.M.*, 1978: Empirical equations for some soil hydraulic properties. *Water Resour. Res. 14*, 601-604.

De Ridder, K. and *Schayes, G.*, 1997: The IAGL land surface model. *J. Appl. Meteor. 36*, 167-183.

Dickinson, R.E., 1984: Modelling evapotranspiration for three dimensional global climate models. In *Climate Processes and Climate Sensitivity* (eds.: *J.E. Hanson* and *T. Takahashi*). *Geophys. Monogr., Amer. Geophys. Union 29*, 58-72.

Entekhabi, D. and *Eagleson, P.S.*, 1989: Land surface hydrology parameterization for atmospheric general circulation models including subgrid scale spatial variability. *J. Climate 2*, 816-831.

Gates, M.D., 1981: *Biophysical Ecology*. Springer Verlag, 339 pp.

Gerwitz, A. and *Page, E.R.*, 1974: An empirical mathematical model to describe plant root system. *J. Appl. Ecol. 11*, 773-782.

Henderson-Sellers, A., Yang, Z.-L. and *Dickinson, R.E.*, 1993: The project for intercomparison of land-surface parameterization schemes. *Bull. Amer. Meteor. Soc. 74*, 1335-1349.

Holtslag, A.A.M. and *Van Ulden, A.P.*, 1983: A simple scheme for daytime estimates of the surface fluxes from routine weather data. *J. Clim. Appl. Meteor. 22*, 517-529.

Jarvis, P.G., 1976: The interpretation of the variations in leaf water potential and stomatal conductance found in canopies in the field. *Philos. Trans. Roy. Soc. London*, Ser.B., 273, 593-610.

Lynn, B.H. and *Carlson, T.N.*, 1990: A stomatal resistance model illustrating plant vs. external control of transpiration. *Agric. and Forest Meteorol. 52*, 5-43.

Noilhan, J. and Planton, S., 1989: A simple parameterization of land surface processes for meteorological models. *Mon. Wea. Rev. 117*, 536-550.

Sellers, P.J. and *Dorman, J.L.*, 1987: Testing the simple biosphere model (SiB) using point micrometeorological and biophysical data. *J. of Clim. Appl. Meteorol. 26*, 622-651.

Sellers, P.J., Mintz, Y., Sud, Y.C. and *Dalcher, A.*, 1986: A simple biosphere model (SiB) for use within general circulation models. *J. Atm. Sci. 43(7)*, 505-531.

Sun, S.F., 1982: Moisture and heat transport in a soil layer forced by atmospheric conditions. *M.S. thesis, Dept. of Civil Engineering, University of Connecticut*, 72 pp.

van der Hornert, T.H., 1948: Water transport as a catenary process. *Discuss. Faraday Soc. 3*, 146-153.

Viterbo, P. and *Beljaars, A.C.M.*, 1995: An improved land-surface parameterization scheme in the ECMWF model and its validation. *J. Climate 8*, 2716-2748.

IDŐJÁRÁS

Quarterly Journal of the Hungarian Meteorological Service
Vol. 102, No. 2, April–June 1998, pp. 129–131

Short Contribution

Effect of potassium chloride (KCl) on plant water status of semi-dry rice at different time of flooding

N. S. Venkataraman, N. Kempuchetty and **S. Mohandass**

Tamil Nadu Rice Research Institute,
Aduthurai 612 101, India

(Manuscript received 26 January 1998)

Abstract—Field experiment was conducted during the wet season of 1994–95 to study the influence of time of submergence and foliar spray of potassium chloride on plant water status and grain yield of semi-dry rice. The results indicated that the foliar spray of 1% potassium chloride (KCl) on the 30th day after sowing (30 DAS) followed by flooding delayed up to 45 and 60 DAS improved the plant water status by means of reduced leaf temperature and transpiration rate.

Key-words: semi-dry rice, submergence, potassium chloride, plant water status, transpiration, leaf temperature, yield.

Semi-dry rice (dry seeded bunded rice) refers to rice which is sown on dry seedbed as an upland crop taking advantage of monsoon rain. At the fourth or fifth leaf stage, when the seasonal rains intensify or sufficient water supply is available from the canal, the field is submerged like wet land rice (*Lubigan and Moody,* 1982). The major barriers of improving the productivity of rice in this system are moisture stress at different growth stages, percolation loss and inefficient use of plant nutrients.

A field experiment was conducted at Tamil Nadu Rice Research Institute, Aduthurai, India during the wet season of August 1994 - January 1995 to study the effect of potassium chloride on plant water status of semi-dry rice (variety CR 1009) at different time of flooding (viz. 30, 45 and 60 DAS). The rice was sown on clay loam soil with pH 7.2 and organic carbon 0.38% while available N, P and K content were 220, 13.8 and 256.2 kg/ha, respectively. Foliar spray of KCl was given on the 30 DAS as drought mitigation. Measurements of transpiration rate, leaf temperature and relative leaf water content were taken

at tenth day after the foliar spray of KCl. Standard errors for mean difference (SE_D) and critical difference (CD) were worked out at 5% probability level (*Gomez* and *Gomez,* 1984).

The results are shown in *Tables 1* and *2*. Adequate supply of potassium during water stress condition made the guard cell turgid around the stomata and led to regulation of transpiration (*Breg,* 1972; *Duraisamy* and *Rosenberg*, 1977). This might be due to increased K ion content, which facilitates water uptake by increasing the osmotic potential of root cells and xylem sap (*Steineck* and *Header*, 1978) under water stress. Potassium has an effect on the maintenance of cell turgidity and helps to reduce the leaf temperature by transpirational cooling of leaves.

Table 1. Effect of time of submergence on semi-dry rice

Submergence	Transpiration (mmol H_2O m^{-2} sec^{-1})	Leaf temperature (°C)	Relative leaf water content (%)	Water use efficiency (kg ha^{-1} mm^{-1})	Dry matter production (kg ha^{-1})	Grain yield (kg ha^{-1})
30 DAS	12.53	26.43	85.16	2.74	10261	4894
45 DAS	11.36	28.78	76.41	2.84	10252	4788
60 DAS	11.10	29.39	75.60	2.67	9418	4255
SE_D	0.26	0.23	0.39	0.03	66	103
CD	0.92	0.63	1.09	0.08	184	286

Table 2. Combined effect of the time of submergence and of KCl on semi-dry rice

	KCl (1%)					
Submergence	Transpiration (mmol H_2O m^{-2} sec^{-1})	Leaf temperature (°C)	Relative leaf water content (%)	Water use efficiency (kg ha^{-1} mm^{-1})	Dry matter production (kg ha^{-1})	Grain yield (kg ha^{-1})
30 DAS	12.11	26.72	88.38	3.25	11337	5830
45 DAS	9.15	26.58	80.65	3.28	11331	5682
60 DAS	9.71	26.92	78.14	3.08	11190	5027
SE_D	0.37	0.49	0.60	0.05	113	153
CD	0.89	1.06	1.40	0.12	256	NS

In agreement with *Ali* (1985) we can say that under water stress condition, KCl spray given on 30 DAS improved the water status of plants by means of reducing the leaf temperature and the transpiration rate for a shorter period. The subsequent flooding on 45 DAS improved the uptake of nutrients and the water use efficiency favouring increased growth and yield in semi-dry direct sown rice.

References

Ali, M., 1985: Effect of presowing seed treatment, foliar nutrition and planting pattern on productivity and water use in chick pea under rainfed condition. *Legume Res. 8*, 7-11.

Breg, H., 1972: The influence of potassium on the transpiration rate and stomatal opening in *Triticum aestivum* and *Pisum sativum*. *Pl. Physiol. 26*, 250-257.

Duraisamy, P.C. and *Rosenberg, N.J.*, 1979: Reflectant induced modification of soybean canopy radiation balance. Preliminary tests with a Kaolinite reflectant. *Agron. J. 86*, 224-228.

Gomez, K.A. and *Gomez, A.A.*, 1984: *Statistical Procedure for Agricultural Research*. John Wiley and Sons, New York.

Lubigan, R.T. and *Moody, K.*, 1982: Herbicide combination for weed control in dry seeded wet land rice in Philippines. In *Proc. Conf. Plant Prot. in Tropics*. Kualalumpur, Malaysia, pp. 511-518.

Steineck, O. and *Header, H.E.*, 1978: The effect of potassium on growth and yield components of plants. In *Potassium Research Review Trends*. International Potash Institute, Switzerland, pp. 165-185.

BOOK REVIEW

M. Yoshino, M. Domrös, A. Douguédroit, J. Paszynski and *L. Nkemdirim* (eds.): **Climates and Societies — A Climatological Perspective**. Kluwer Academic Publishers, Dodrecht, Boston, London, 1997. 11 + 408 pages, 127 figures, 42 tables and several photos.

In the 1970s a comprehensive scientific activity began related to the impact of climate on human life and the effect of humans on climate. Series of international cooperations were organized, like World Climate Programme (WCP), International Geosphere-Biosphere Programme (IGBP). Intergovernmental Panel on Climate Change (IPCC), Working Group on Tropical Climatology and Human Settlements, International Association on Meteorology and Physics (IAMAP), etc. These wide international cooperations have stored up a great deal of new scientific informations and knowledges, partly published in different periodicals and journals.

This book is written by some of the world's leading climatologists and environmental scientists. It addresses many of issues raised in the debate on global change, providing new insights into climate and its integration into space and time organizations of societies. The volume contains three main parts:

(1) Climatic changes and variability.
(2) Climate on regional scale including climate related problems in major climatic regions ranging from tropics through the temperate zone to the Poles.
(3) Human-climate relationships on local scale.

The introduction was written by *Masatoshi Yoshino*. The first greater part consists of 6 chapters written by *A. Douguédroit; J. Zhang, Y. Yasuda* and *M. Yoshino; Fr. Serre-Bachet; C. D. Schönwiese; H. Le Treut; A. Douguédroit, J.-P. Marchand, M.-F. de Saintignon* and *A. Vidal*.

The introduction, entitled "Human activities and environmental change: a climatologist's wiew", presents data on emissions of greenhouse gases in several countries of Asia, Australia and the Philippines. The author emphasizes the importance of environmental education and outlines the changes in ecosystems, agricultural products, sea level.

Chapter 2.1 (Climate variability and societies) presents two approaches of climate: a physical and a social approach. Among others the reader encounters problems of telecommunication and ENSO events in this chapter. Chapter 2.2 (Climate change in post glacial period in monsoon Asia) is remarkable as far as the warm/cold or wet/dry periods in the last 18000-year period are

considered. Climatic information sources and climate reconstruction methods are the subjects of Chapter 2.3 (Approaches to climatic variations during the historical era). The next chapter (2.4) deals with some statistical aspects of observed regional and global climate change within the instrumental period including autocorrelation spectral analysis, maximum entropy spectral analysis and so forth.

Chapter 2.5 (Climate of the future: on evaluation of the current uncertainties) gives a good review on achievements of the IPCC researches. Chapter 2.6 (Impacts on the climate variability on human activities) is a comprehensive summary of the topic.

The next great part, entitled "Regional Scales Climates" consists of Chapters 3.1–3.7 and deals with topics like society-climate systems in tropical Africa, climate and life in the Caribbean Basin, climate and societies in Southeast Asia, climatic and pathological rhythms in a humid tropical area (the case of the Philippines), possible impact of the climatic change and variability on agriculture in South America, climate and agriculture in China and the climates of the polar regions.

The last part, "Local scale climates" including Chapters 4.1–4.5, gives reviews on problems of local climate and man, namely on interactions of man and climate in urban world, the influence of urbanisation on the local climate and the influence of urban climate on man, climates of tropical and subtropical societies, air pollution (a local problem becomes a global problem), agricultural landuse and local climate.

The authors of these chapters are as follows: *O. Ojo; L. C. Nkemdirom; K.U. Sirinanda; J. Pérard* and *J.-P. Besancenot; F.- Santibañez; A.-L. Jiang; T. Niedzwiedz; J. Paszynski; F. Wilmers; E. Jauregui; H. Wanner; M. Yoshino*.

Besides the great variety of subjects, this book provides numerous sources of up-to-date knowledge on past, present and future climates, their problems and impacts.

G. Koppány

NEWS

BSRN 5th Science and Review Workshop

The BSRN (Baseline Surface Radiation Network) is one of the subprogrammes of WCRP (World Climate Research Programme). Its purpose is to establish 20–30 surface radiometric stations to provide most reliable radiation data for

- deriving of climatic trends in radiation parameters;
- validating of surface radiation products derived from satellite measurements.

The BSRN started in 1988 in Würzburg (Germany). The 5th Workshop was held in Budapest from 18 to 22 May, 1988. The objective of this workshop was to bring BSRN scientists, station managers, data users and experts in areas related to BSRN activities together to review

- the status of the implementation of the network;
- the latest developments in instrumentation and operational procedures, data management and quality control;

to discuss some of the scientific progresses achieved as a result of availability of the BSRN data archive; and to consider future needs and plans for the BSRN.

The meeting was attended by 43 participants, the largest number in the history of BSRN workshops. The participants presented nearly 20 station status reports and more than 20 technical and scientific reports.

The longest discussion was paid to the "BSRN Operations Manual (Version 1.0)" compiled by *Dr. Bruce McArthur* (Canada). This manual will be available at the WCRP Office's web site. It contains sections on sampling frequency and accuracy requirements for BSRN stations, the siting of the stations, the installation of radiation instruments, solar tracking devices, data acquisition, station maintenance, radiation instrument calibration, radiation data reduction and quality assurance procedures as well as a variety of ancillary information in the annexes.

The BSRN Working Group approved a 4-page document entitled: "BSRN data release policy". It was compiled by a subgroup that had been nominated during the 1996 meeting in Boulder (USA). The basic idea is to defend the interests of the station scientists who produce the data.

Other items addressed during the meeting:

- aerosol optical depth,
- geometry of pyrheliometers and diffusometers,

- all-weather cavity pyrheliometers,
- UV-B measurements, liaison to GAW program,
- pyranometer offsets,
- photosynthetically active radiation,
- complete literature search for existing published papers on the performance and characteristics of thermopile based radiometers used for solar and terrestrial irradiance measurements,
- albedo and surface properties,
- longwave irradiance reference,
- longwave data reduction,
- shortwave leak in pyrgeometer domes,
- cloud base height,
- pyrgeometer characterization, calibration and classification.

A comprehensive report on this BSRN meeting will be compiled by *Roger Newson* and *Hans Teunissen* (WCRP Office) and it will be published by the WMO in the second half of 1998.

The next workshop is planned for the year of 2000.

Major György

ATMOSPHERIC ENVIRONMENT

an international journal

To promote the distribution of Atmospheric Environment *Időjárás* publishes regularly the contents of this important journal. For further information the interested reader is asked to contact *Prof. P. Brimblecombe*, School for Environmental Sciences, University of East Anglia, Norwich NR4 7TJ, U.K.; E-mail: atmos_env@uea.ac.uk

Volume 32 Number 3 1998

International Conference on Atmospheric Ammonia: Emission, Deposition and Environmental Impacts

Biosphere-atmosphere exchange

D.S. Lee, C. Halliwell, J.A. Garland, G.J. Dollard and *R.D. Kingdon:* Exchange of ammonia at the sea-surface – a preliminary study, 134-439.

G.P. Wyers and *J.W. Erisman:* Ammonia exchange over coniferous forest, 441-451.

D. Fowler, C.R. Flechard, M.A. Sutton and *R.L. Storeton-West:* Long-term measurements of the land-atmosphere exchange of ammonia over moorland, 453-459.

Canopy exchange processes and physiological control of ammonia fluxes

J.K. Schjoerring, S. Husted and *M. Mattsson:* Physiological parameters controlling plant-atmosphere ammonia exchange, 491-498.

A. Neftel, A. Blatteeer, A. Gut, D. Högger, F. Meixner, C. Ammann and *F.J. Nathaus:* NH_3 soil and soil surface gas measurements in a triticale wheat field, 499-505.

J.K. Schjoerring, S. Husted and *M.M. Poulsen:* Soil-plant-atmosphere ammonia exchange associated with *Calluna vulgaris* and *Deschampsia flexuosa*, 507-512.

Impacts of ammonia and ammonium deposition

L. van der Eerden, W. De Vries and *H. van Dobben:* Effects of ammonia deposition on forests in The Netherlands, 525-532.

J. Pearson and *A. Soares:* Physiological responses of plant leaves to atmospheric ammonia and ammonium, 533-538.

Z.H. Yin, W. Kaiser, U. Heber and *J.A. Raven:* Effect of gaseous ammonia on intracellular pH values in leaves of C_3- and C_4-plants, 539-544.

Critical loads and ammonia control policies

K.R. Bull and *M.A. Sutton:* Critical loads and the relevence of ammonia to an effects-based nitrogen protocol, 565-572.

D.A. Cowell and *H.M. Apsimon:* Cost-effective strategies for the abatement of ammonia emissions from European agriculture, 573-580.

L.J.A. Lekkerkerk: Implications of Dutch ammonia policy on the livestock sector, 581-587.

Volume 32 Number 4 1998

G. Drakou, C. Zerefos, I. Ziomas and *M. Voyatzaki:* Measurements and numerical simulations of indoor O_3 and NO_x in two different cases, 595-610.

R.J. Brown and *R.W. Bilger:* Experiments on a reacting plume–1. Convertional concentration statistics, 611-628.

R.J. Brown and *R.W. Bilger:* Experiments on a reacting plume–2. Conditional concentration statistics, 629-646.

Alexey Ryaboshapko, Laura Gallardo, Erik Kjellström, Sergey Gromov, Sergey Paramonov, Olga Afinogenova and *Henning Rodhe:* Balances of oxidized sulfur and nitrogen over the former Soviet Union territory, 647-658.

Juão F.P. Gomes: Assessment of opacimeter calibration on kraft pulp mills, 659-664.

Robert L. Lee and *Erik Näslund:* Lagrangian stochastic particle model simulations of turbulent dispersion around buildings, 665-672.

L. Cheng, K.M. McDonald, R.P. Angle and *H.S. Sandhu:* Forest fire enhanced photochemical air pollution. A case study, 673-681.

Volume 32 Number 5 1998

Atmospheric Transport, Chemistry and Deposition of Mercury

Volume 32 Number 6 1998

NOTES TO CONTRIBUTORS OF *IDŐJÁRÁS*

The purpose of the journal is to publish papers in any field of meteorology and atmosphere related scientific areas. These may be

- reports on new results of scientific investigations,
- critical review articles summarizing current state of art of a certain topic,
- shorter contributions dealing with a particular question.

Each issue contains "News" and "Book review" sections.

Authors may be of any nationality, but the official language of the journal is English. Papers will be reviewed by unidentified referees.

Manuscripts should be sent to
Editor-in-Chief of IDŐJÁRÁS
P.O. Box 39
H-1675 Budapest, Hungary

in three copies including all illustrations. One set of illustrations has to be of camera ready quality, the other two might be lower quality.

Title part of the paper should contain the concise title, the name(s) of the author(s), the affiliation(s) including postal and E-mail address(es). In case of multiple authors, the cover letter should indicate the corresponding author.

Abstract should follow the title, it contains the purpose, the data and methods as well as the basic conclusion.

Key-words are necessary to help to classify the topic.

The text has to be typed in double spacing with wide margins. Word-processor printing is preferred. The use of SI units are expected. The negative exponent is preferred to solidus. Figures and tables should be consecutively numbered and referred to in the text.

Mathematical formulas are expected to be as simple as possible and numbered in parentheses at the right margin. Non-Latin letters and hand-written symbols should be indicated and explained by making marginal notes in pencil.

Tables should be marked by Arabic numbers and printed in separate sheets together with their captions. Avoid too lengthy or complicated tables.

Figures should be drawn or printed in black and white, without legends, on separate sheets. The legends of figures should be printed as separate list. Good quality laser printings are preferred as master copies.

References: The text citation should contain the name(s) of the author(s) in Italic letter and the year of publication. In case of one author: *Miller* (1989), or if the name of the author cannot be fitted into the text: *(Miller,* 1989); in the case of two authors: *Gamov* and *Cleveland* (1973); if there are more than two authors: *Smith et al.* (1990). When referring to several papers published in the same year by the same author, the year of publication should be followed by letters a,b etc. At the end of the paper the list of references should be arranged alphabetically. For an article: the name(s) of author(s) in Italics, year, title of article, name of journal, volume number (the latter two in Italics) and pages. E.g. *Nathan, K.K.,* 1986: A note on the relationship between photosynthetically active radiation and cloud amount. *Időjárás 90*, 10-13. For a book: the name(s) of author(s), year, title of the book (all in Italics except the year), publisher and place of publication. E.g. *Junge, C. E.,* 1963: *Air Chemistry and Radioactivity*. Academic Press, New York and London.

The final version should be submitted on diskette altogether with one hard copy. Use standard 3.5" or 5.25" DOS formatted diskettes. The preferred word-processors are WordPerfect 5.1 and MS Word 6.0.

Reprints: authors receive 30 reprints free of charge. Additional reprints may be ordered at the authors' expense when sending back the proofs to the Editorial Office.

More information: gmajor@met.hu
Information on the last issues:
http://www.met.hu/firat/ido-e.html

Published by the Hungarian Meteorological Service

Budapest, Hungary

INDEX: 26 361

HU ISSN 0324-6329